

Sliced Beam Parameter Measurements

D. Alesini (LNF-INFN, Frascati, Rome)

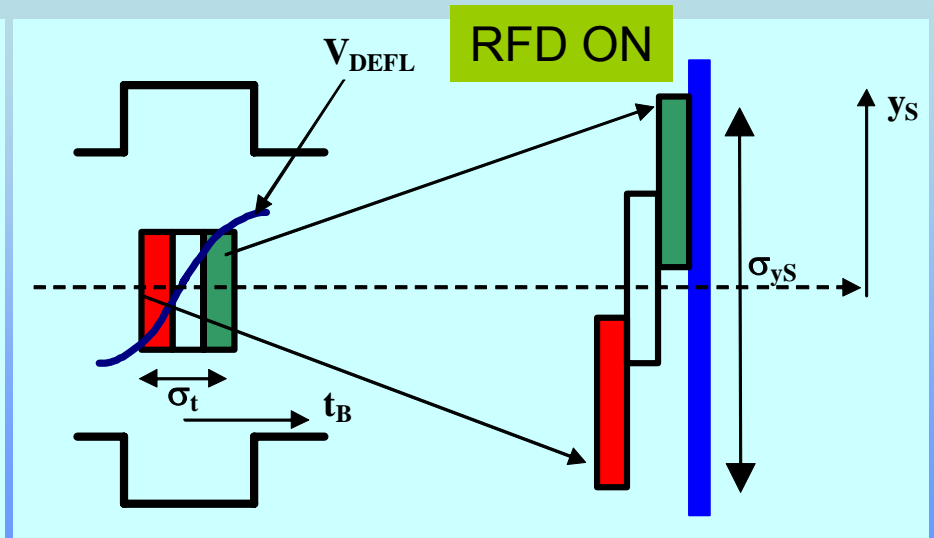
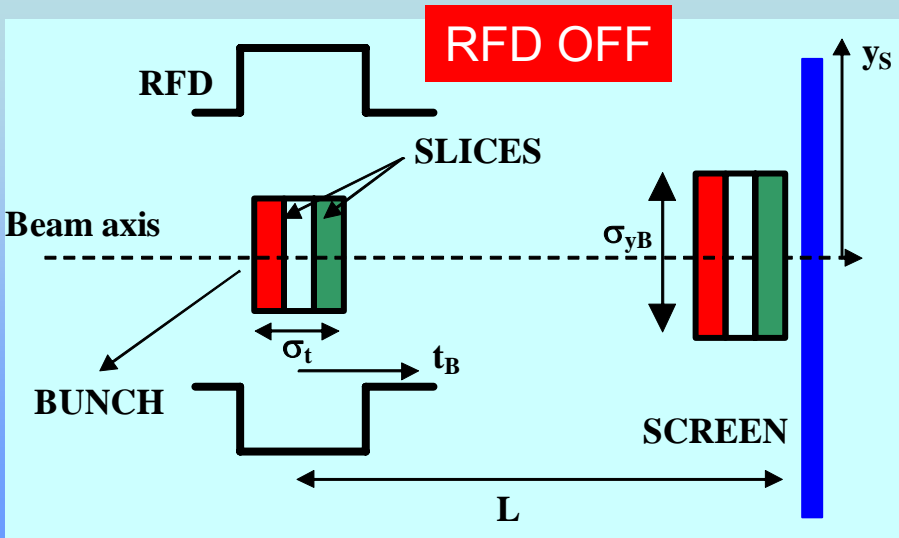
on behalf of the team

B. Marchetti, A. Cianchi (University of Rome Tor Vergata and INFN-Roma Tor Vergata)
E. Chiadroni, M. Castellano, L. Cultrera, G. Di Pirro, M. Ferrario, D. Filippetto, G. Gatti, E. Pace, C. Vaccarezza,
C. Vicario (INFN/LNF, Frascati, Italy)
L. Ficcadenti, A. Mostacci (University La Sapienza, Roma)
C. Ronsivalle (ENEA C.R. Frascati, Italy)

OUTLINE

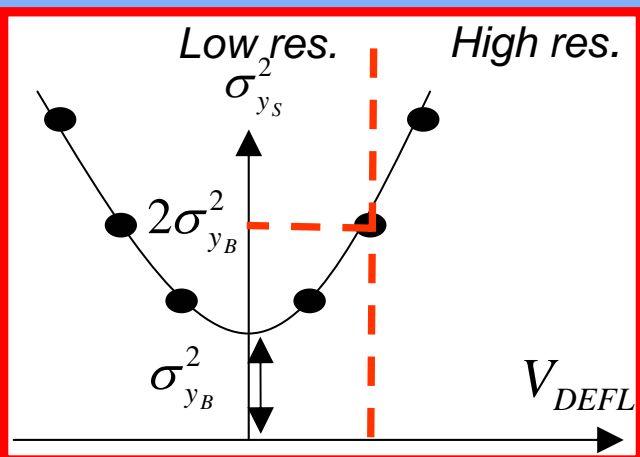
- **Slice parameter measurements by RFD: principle and calibration**
- **RF Deflecting structures:**
 - TW and SW
 - performances
 - transport matrix of a single cell
- **General measurement setup:**
 - beam profile and transverse slice emittance
 - longitudinal phase space
- **SPARC measurement results**
- **LCLS and FLASH results**
- **Advanced RFD structures for beam diagnostics and new proposals**

Slice parameter measurements by RFD: principle



The different types of measurements that can be done with RFDs are based on the property of the transverse voltage (V_{DEFL}) to introduce a **linear correlation between the longitudinal coordinate of the bunch (t_B) and the transverse one** (vertical, in general) at the screen position (y_S).

$$y_S \cong \underbrace{\left(\frac{V_{DEFL}}{E/e} \omega_{RF} L \right)}_{K_{cal}} \left(t_B + \frac{\Delta\phi_{RF}}{\omega_{RF}} \right) + y_B$$



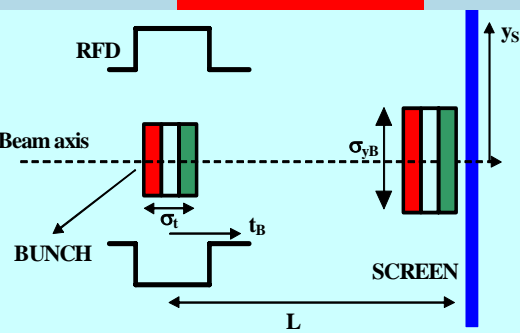
$$\sigma_{yS}^2 \cong K_{cal}^2 \sigma_{tB}^2 + \sigma_{yB}^2$$

resolution

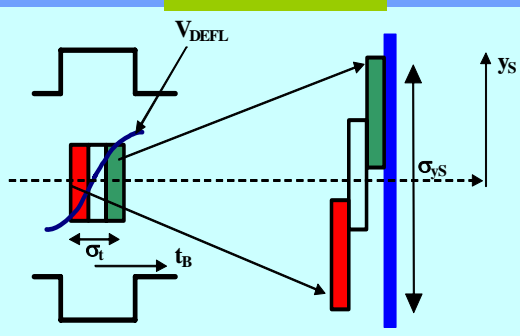
$$\sigma_{tB-RES} = \frac{\sigma_{yB}}{K_{cal}} = \frac{\sigma_{yB}}{\frac{V_{DEFL}}{E/e} \omega_{RF} L}$$

Calibration: measurements @ SPARC

RFD OFF



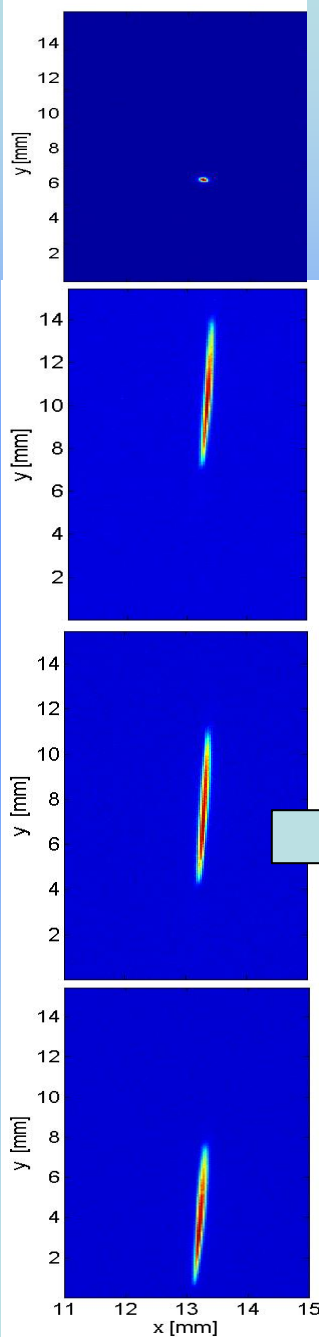
RFD ON



$$K_{cal} \cong \omega_{RF} \frac{\langle y_s \rangle|_{meas_1} - \langle y_s \rangle|_{meas_2}}{\Delta \phi|_{meas_1} - \Delta \phi|_{meas_2}}$$

Self calibrated meas.

The coefficient K_{cal} can be directly calculated measuring the bunch centroid position on the screen for different values of the RFD phase

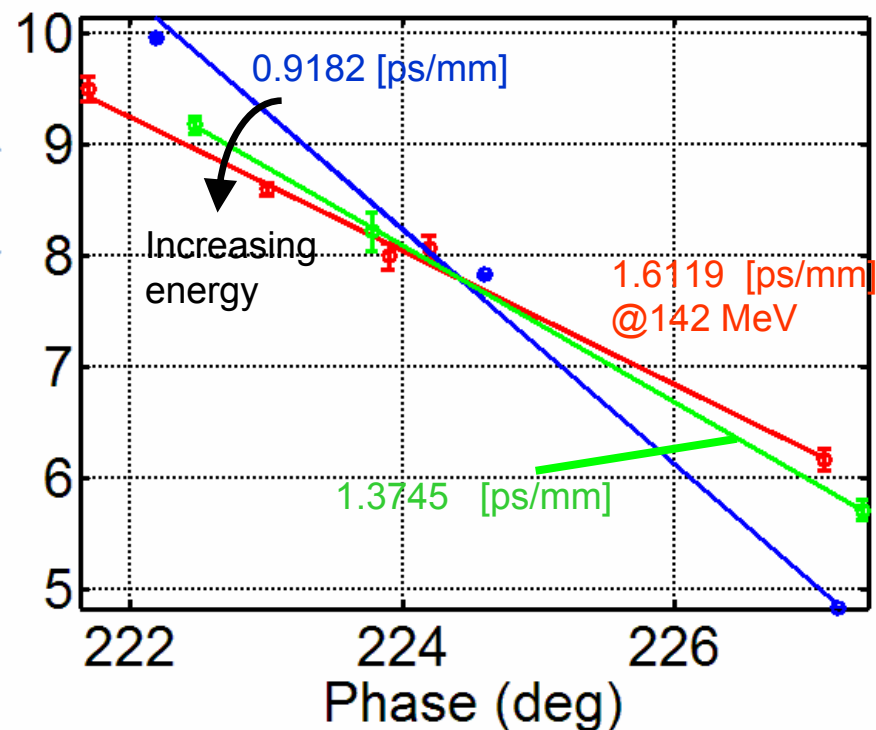


$$\begin{aligned} \sigma_{y_B} &\cong 100 \mu m \\ V_{DEFL} &\cong 1.5 MV \\ E &\cong 150 MeV \\ f_{RF} &\cong 2.856 GHz \\ L &\cong 4 m \end{aligned}$$

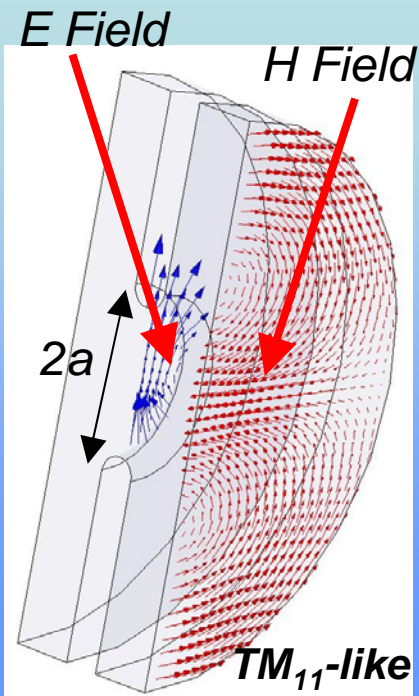
Typical
SPARC
parameters

$$\sigma_{t_B-RES} = \frac{\sigma_{y_B}}{\frac{V_{DEFL}}{E/e} \omega_{RF} L} \cong 130 fs$$

SPARC results @ different energies



RF Deflecting structures: TW case

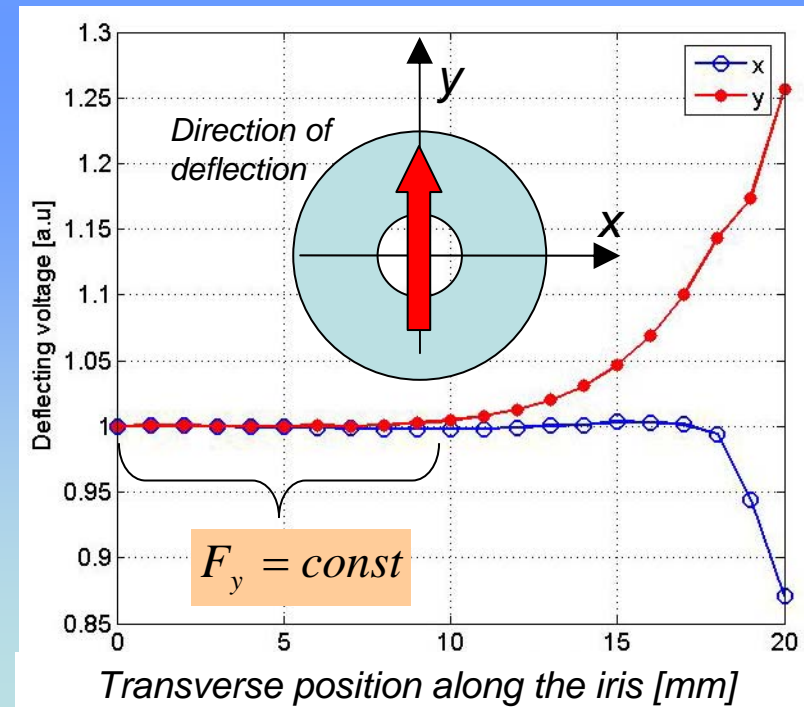
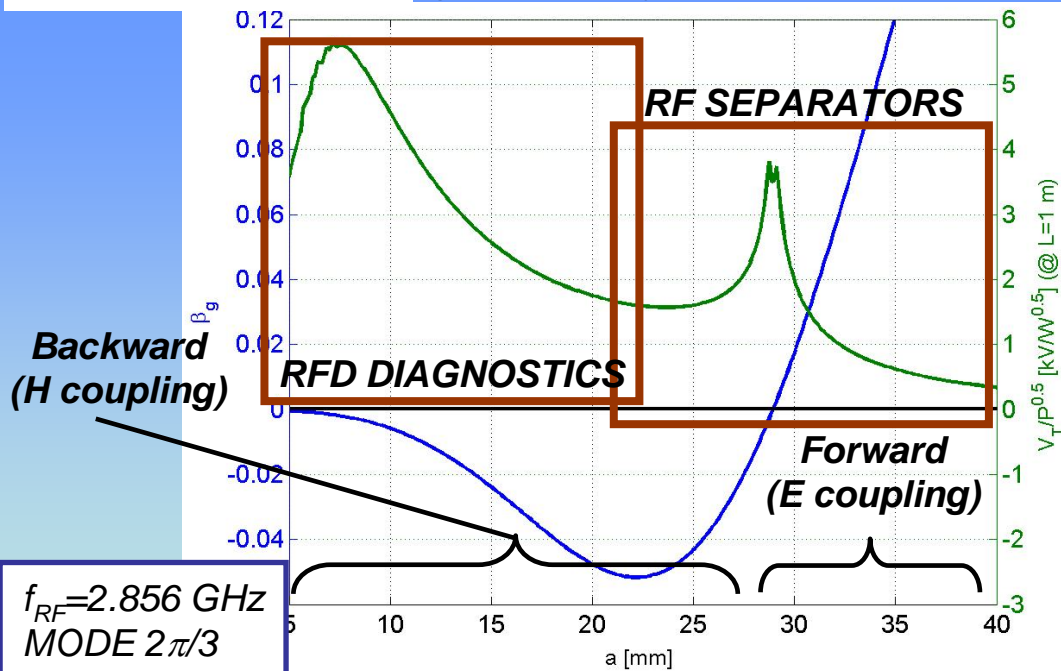
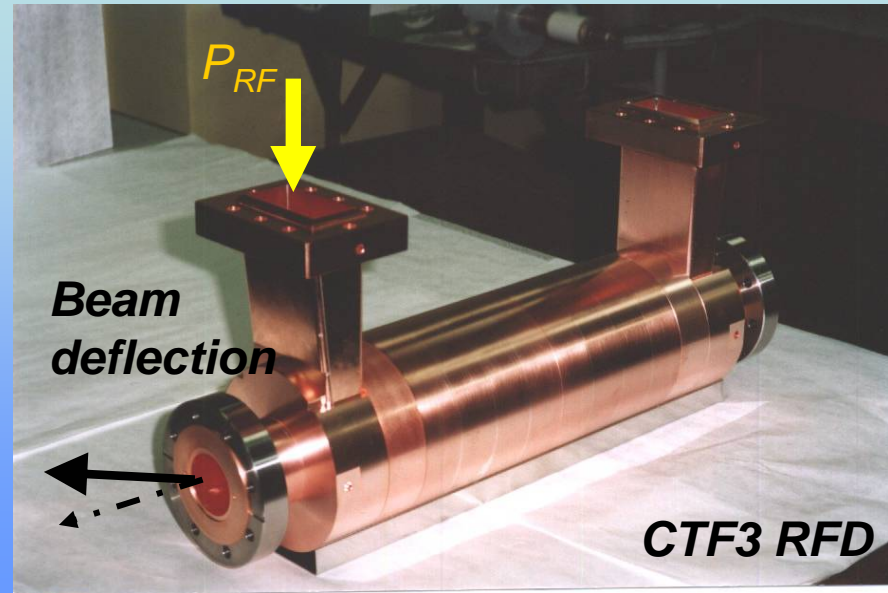


As in the case of accelerating sections, we have **TW and SW cavities**. In general RFDs are multi-cell devices working on the TM11-like mode.

Both the **E** and the **B** field contribute to the total deflection.

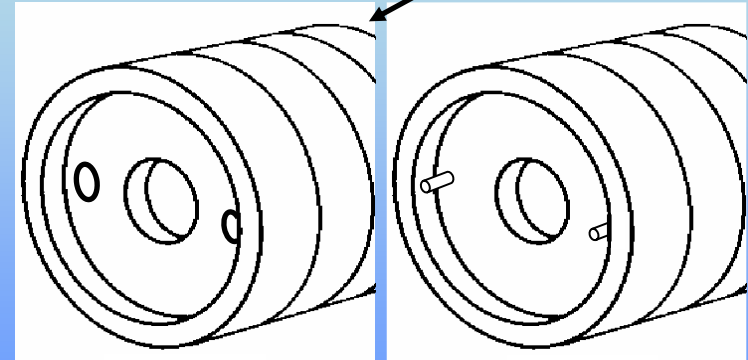
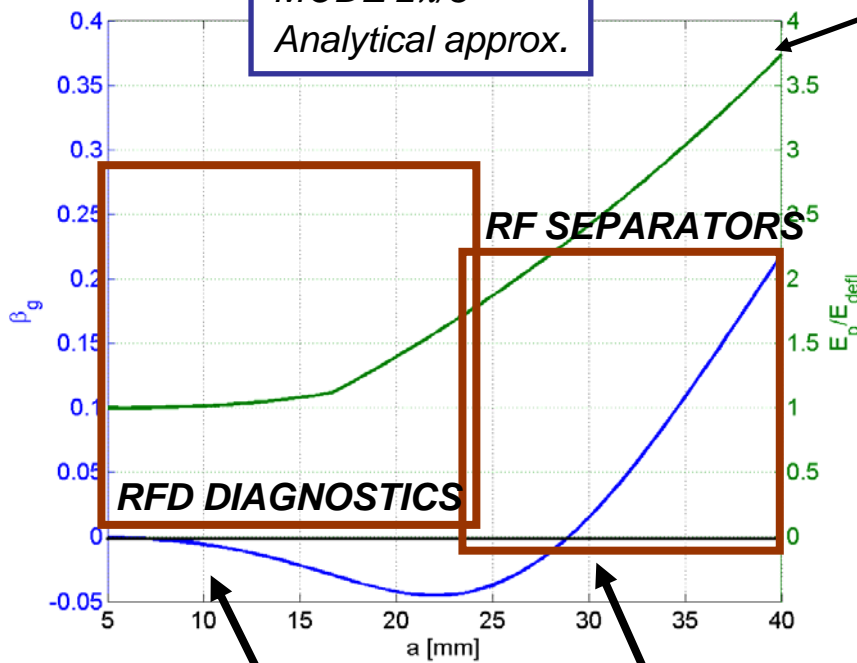
The **transverse force is uniform** over a wide region inside the iris aperture

In TW devices the **iris aperture (a)** is the most important parameter to fix the deflection efficiency and group velocity



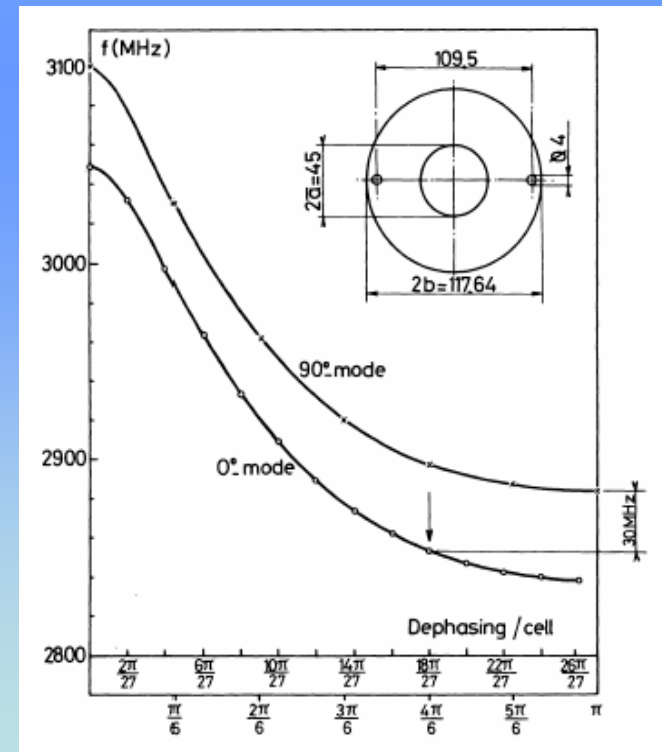
RF Deflecting structures: peak E field and polarization

$f_{RF}=2.856$ GHz
MODE $2\pi/3$
Analytical approx.

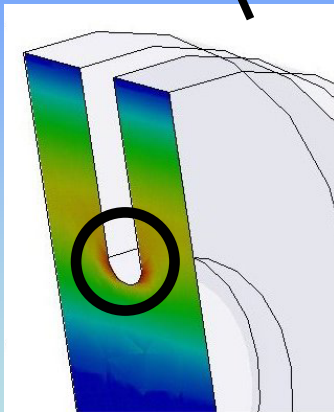
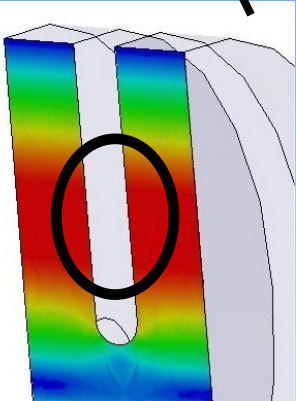


Holes

Rods

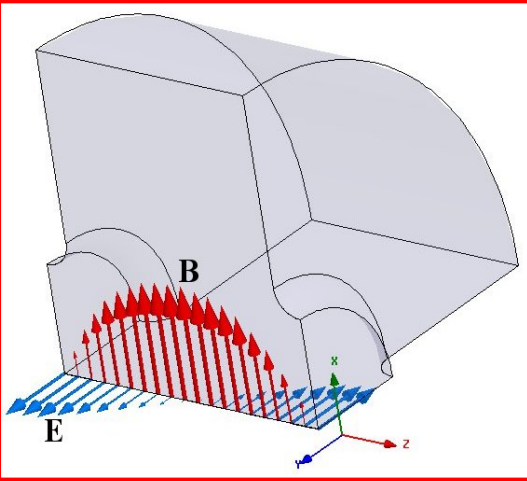


Since there are two possible polarities of the deflecting field, **polarizing rod or holes** are, in general, foreseen to introduce an **azimuthal asymmetry** in the structure fixing the working polarity itself

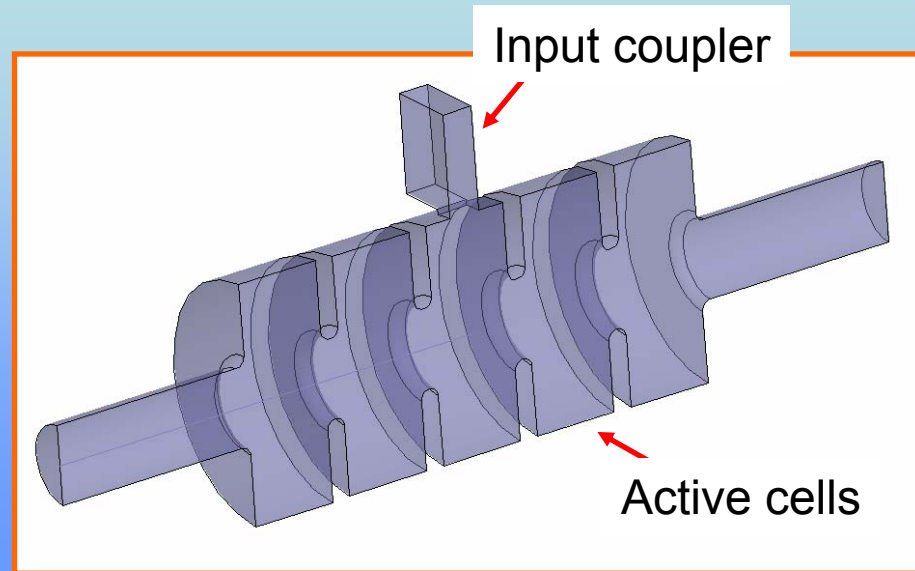


RF Deflecting structures: SW case (SPARC RFD)

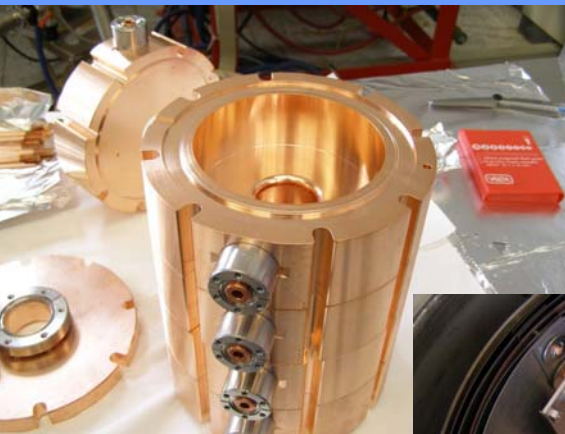
E, B field profiles



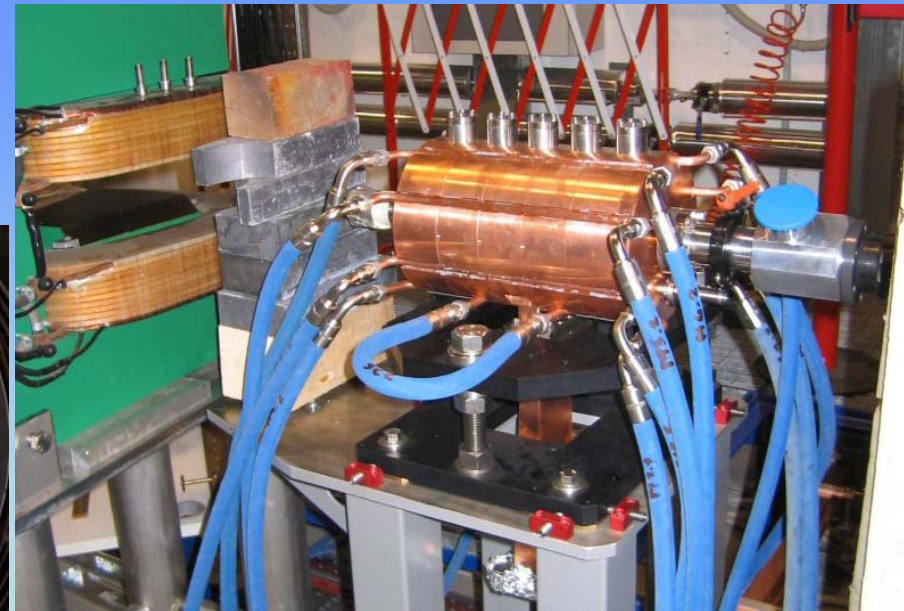
SW structures are multi cell devices working, for example, on the π -mode. These structures have, in general a **higher efficiency per unit length** with respect to the TW ones but the maximum number of cells is limited to few tens because of mode overlapping. They requires **circulators** to protect the RF source from reflections.



RFD installed in SPARC



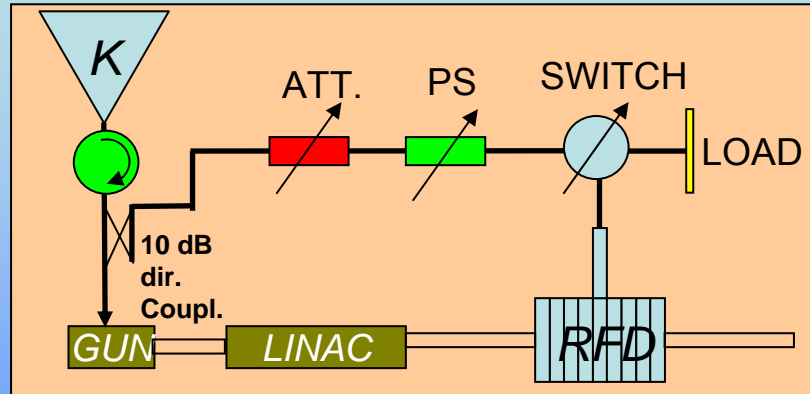
RFD in the LNF oven



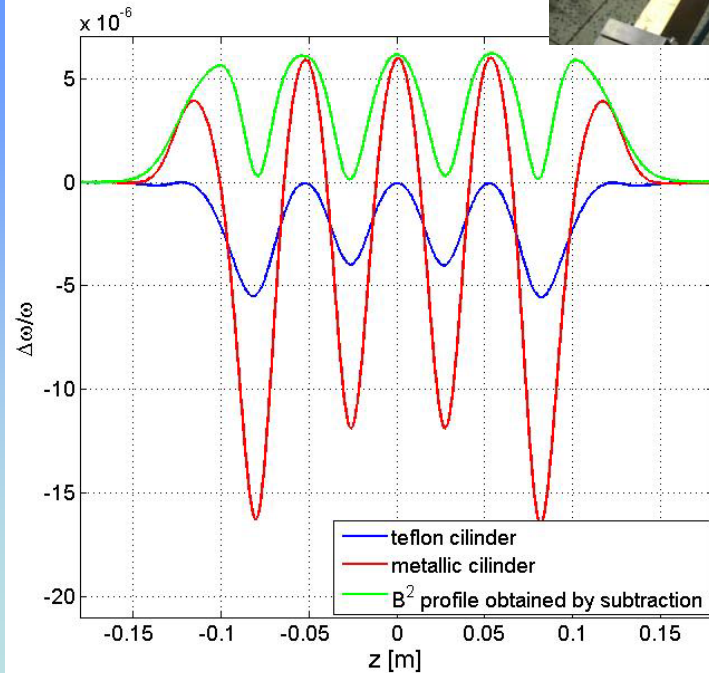
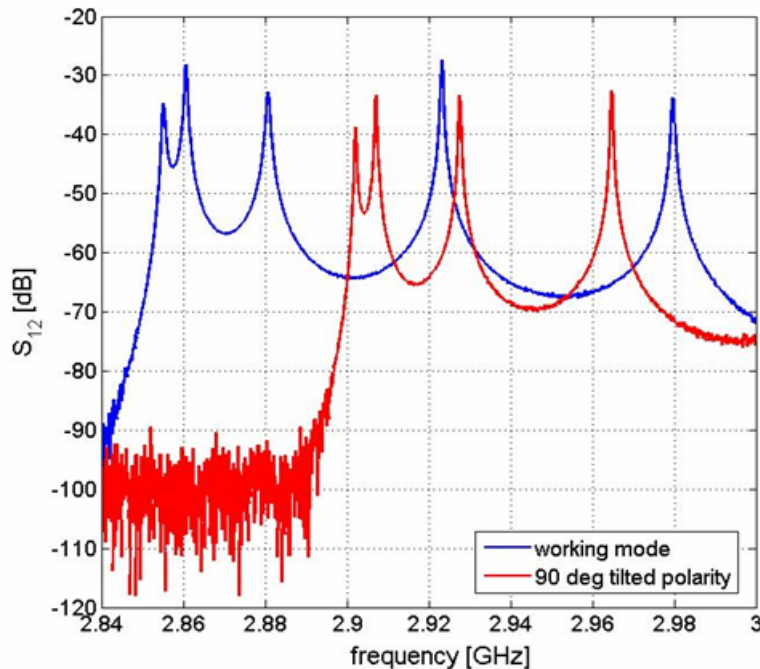
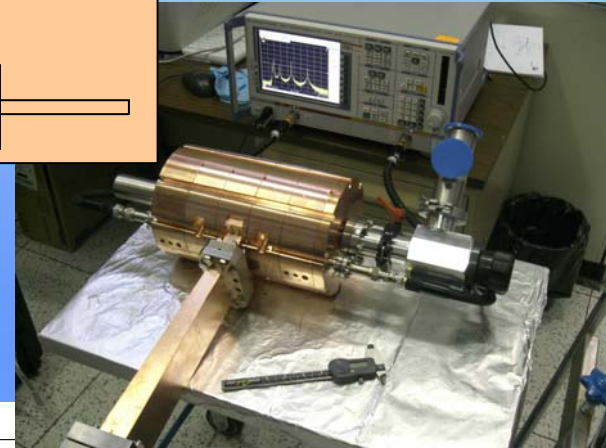
SPARC RF Deflector

PARAMETERS

Deflecting mode	SW, π
Number of cells	5
Frequency	2.856 GHz
Quality factor (Q_0)	16000
Coupling coefficient (β)	1
Max. input power (P_{RF_MAX})	2 MW
Transv. shunt imp. (R_T)	2.4 M Ω
Defl. voltage @ P_{RF_MAX} (V_T)	3 MV
Max. surf. E field (E_{PEAK})	50 MV/m



An example of SW structure is the SPARC RFD. It is a 5 cells SW structure working on the π -mode at 2.856 GHz and fed by a central coupler with coupling coefficient equal to 1.



RF Deflecting structures: performances

$$\varepsilon_N = 1 \text{ [mm*mrad]}$$

$$f_{RF} = 2.856 \text{ [GHz]}$$

$$\beta_S = 1 \text{ m}$$

$$\Rightarrow \sigma_{yB} \approx 18 \text{ } \mu\text{m} \text{ (@1.5 GeV)}$$

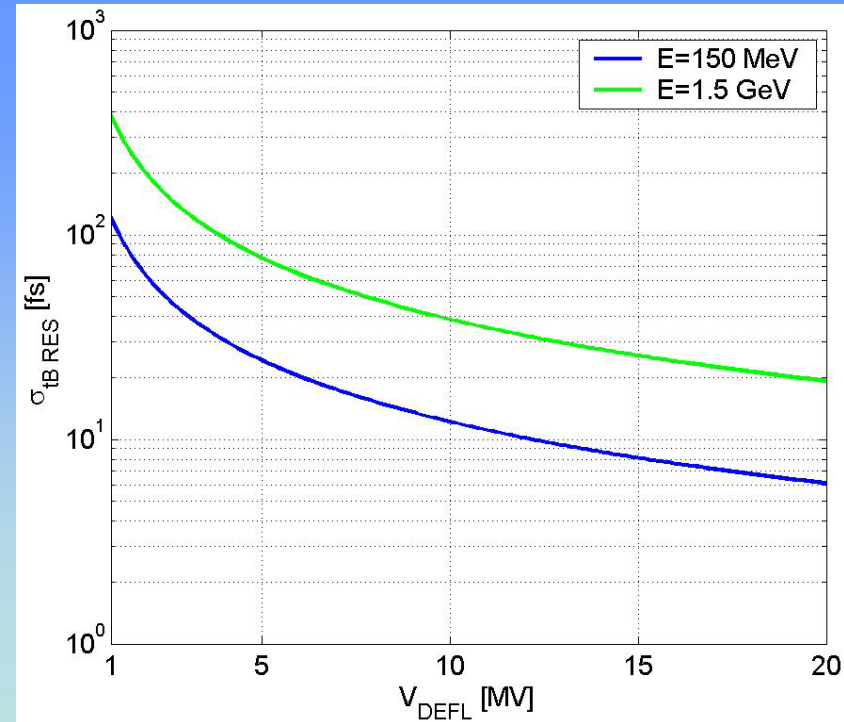
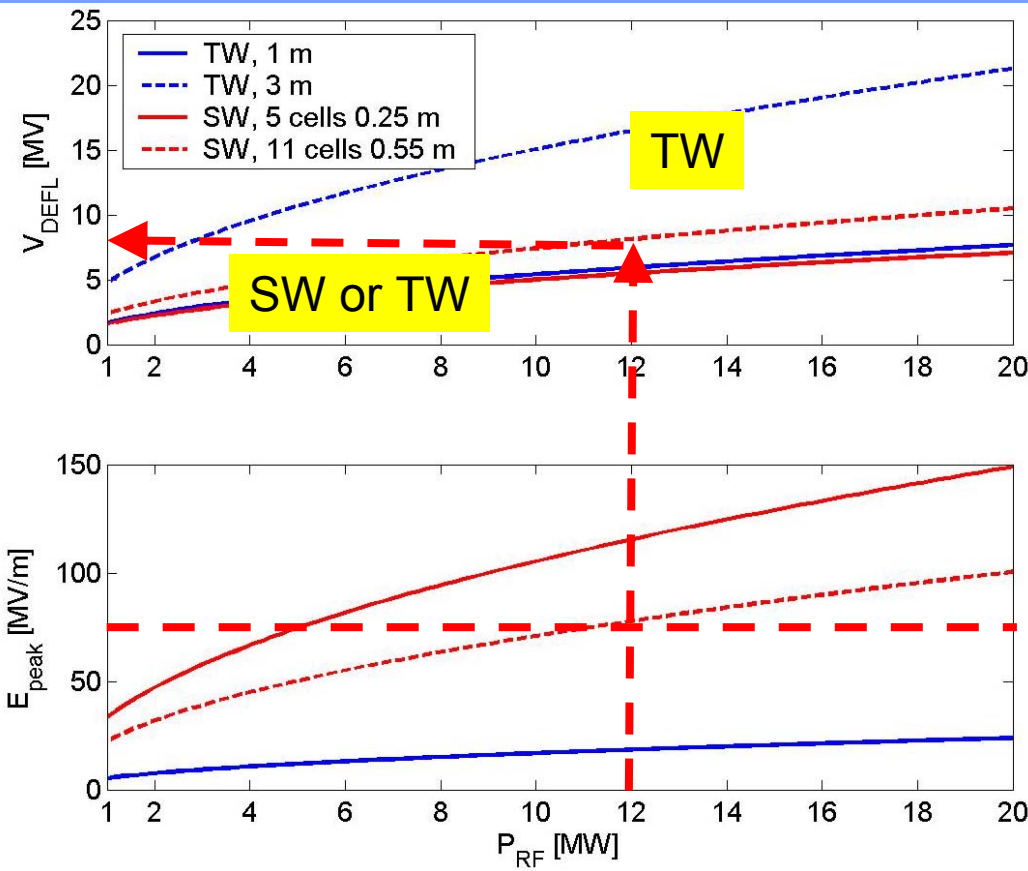
$$\Rightarrow \sigma_{yB} \approx 58 \text{ } \mu\text{m} \text{ (@150 MeV)}$$

$$L_{\text{Defl-Screen}} = 4 \text{ m}$$

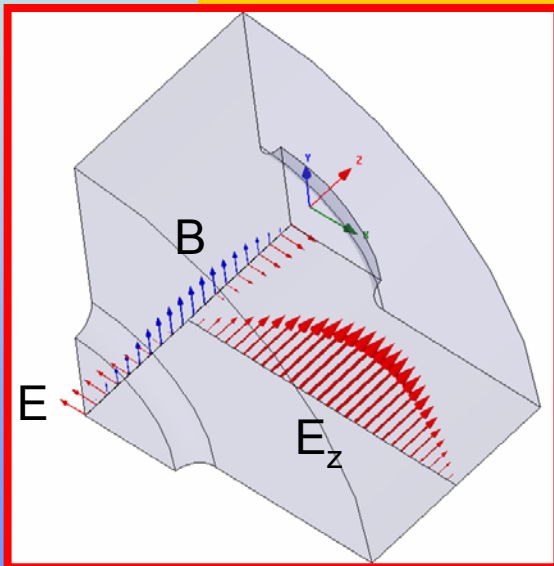
$$\sigma_{t_B - RES} = \frac{\sigma_{y_B}}{\frac{V_T}{E/e} \omega_{RF} L} = \sqrt{E/E_0} \frac{\sqrt{\varepsilon \beta_S}}{V_T \omega_{RF} L}$$

Because of the higher surface electric field, SW multi-cell devices can be used with input power below 10 MW giving $V_{DEFL} < 7 \text{ MV}$

	SW	TW
Efficiency per unit length	High	Low
Filling time	slow	fast
Maximum number of cells	15	3-4 m
Circulator	yes	not
E_{PEAK}	high	low
Beam impact	low	High



RF Deflecting structures: induced energy spread

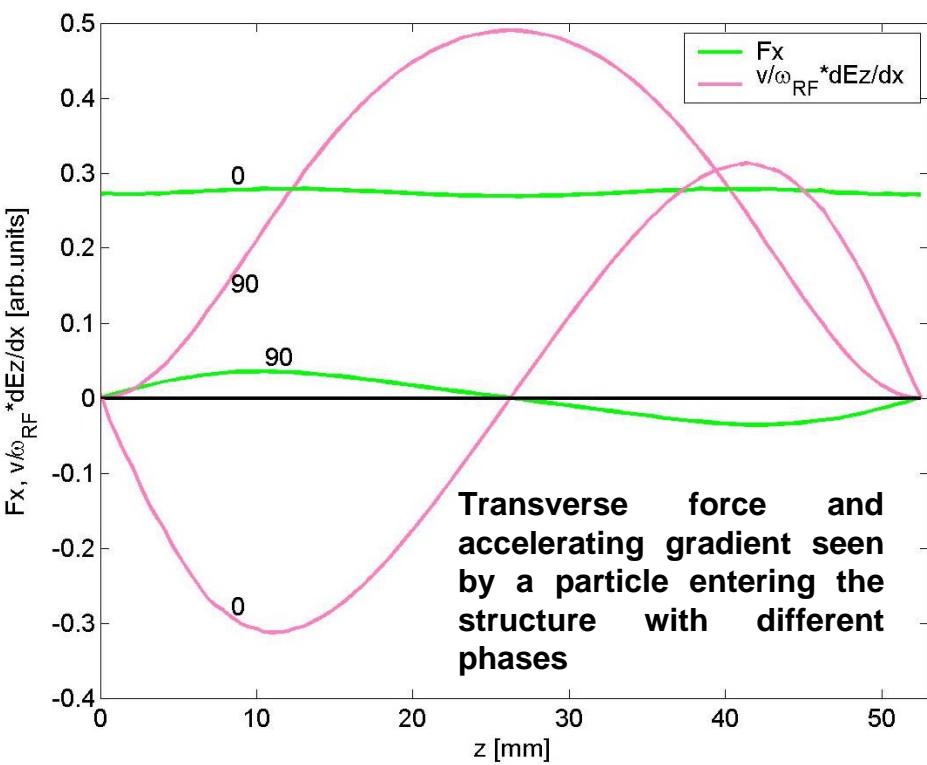
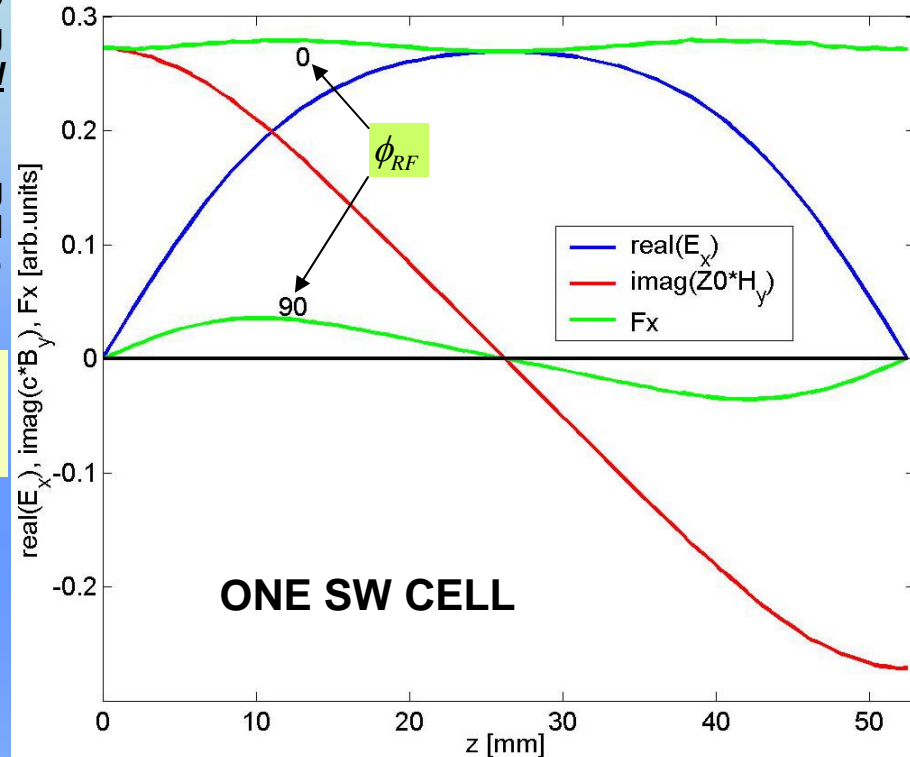


a) The Panofsky-Wenzel theorem relates the RFD transverse deflecting voltage and the longitudinal electric field gradient;

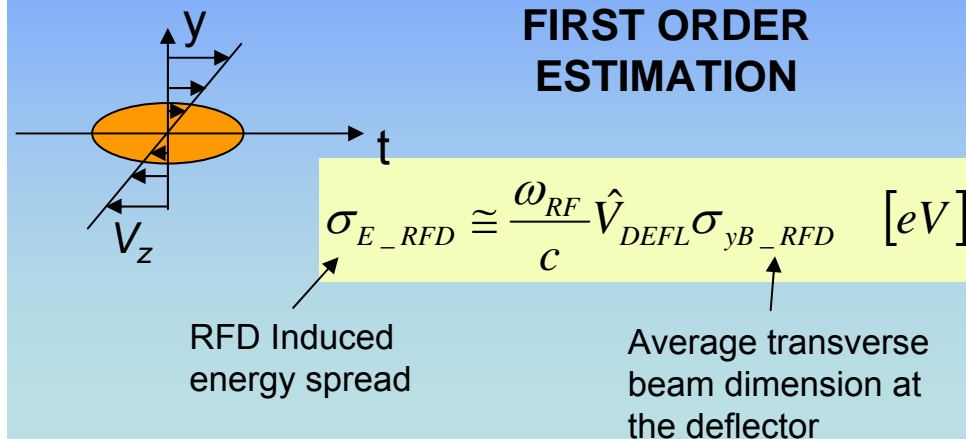
b) The transverse deflecting voltage and the longitudinal one are 90 deg out-of-phase

$$\tilde{V}_{y_RFD} = j \frac{c}{\omega_{RF}} \nabla_y \tilde{V}_{z_RFD}$$

Transverse force and deflecting field components



FIRST ORDER ESTIMATION



RF Deflecting structures: transport matrix of a single cell

RFD Correlation $t_B(y_{OUT}, y'_{OUT})$
allowing the measurements

$$B = -\frac{E_{defl} \omega_{RF}}{E_B} \sin(\phi_{RF})$$

$$E_{defl} = \frac{V_{defl}}{L_{RFD}}$$

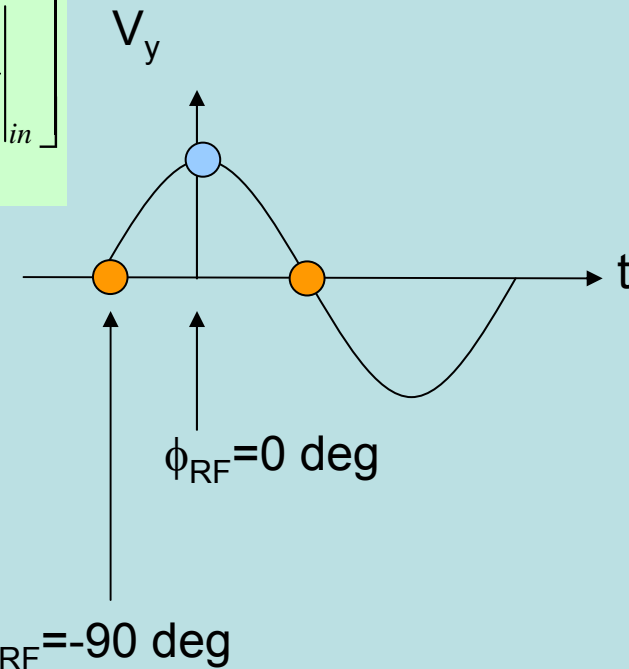
Dispersion terms given by the RFD deflecting
voltage if we are on crest ($\phi_{RF}=0\text{deg}$)

$$C = \frac{E_{defl}}{E_B} \cos(\phi_{RF})$$

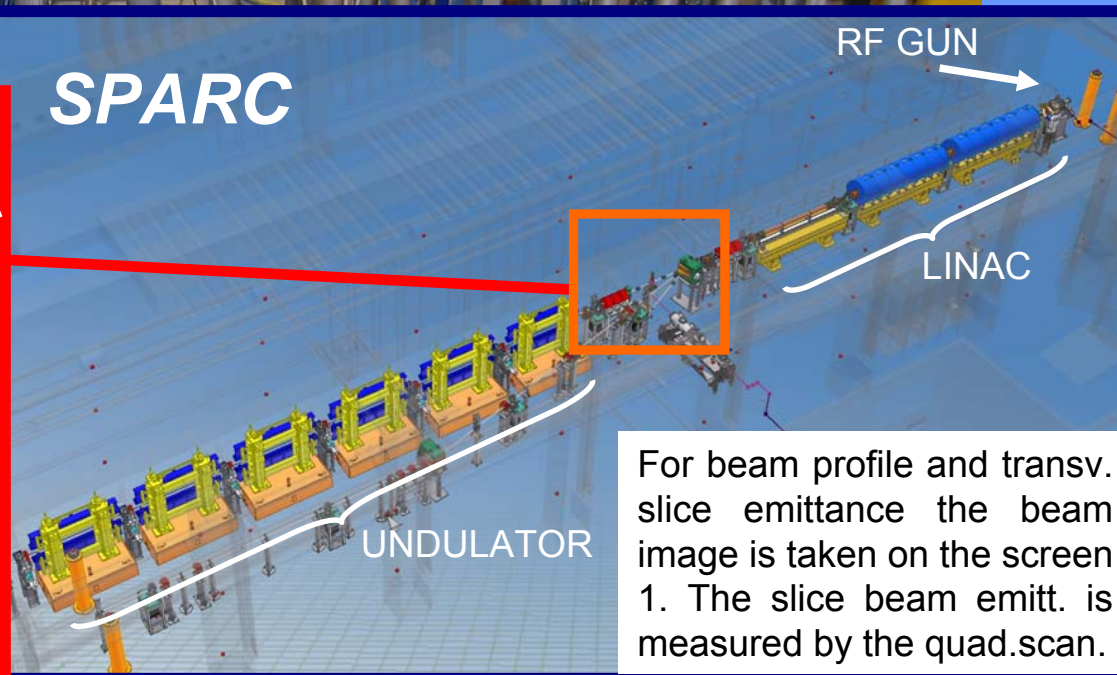
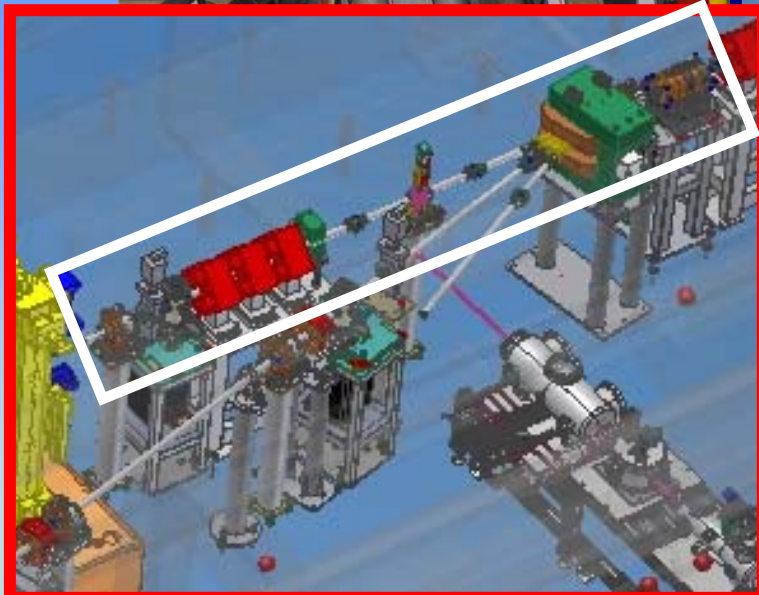
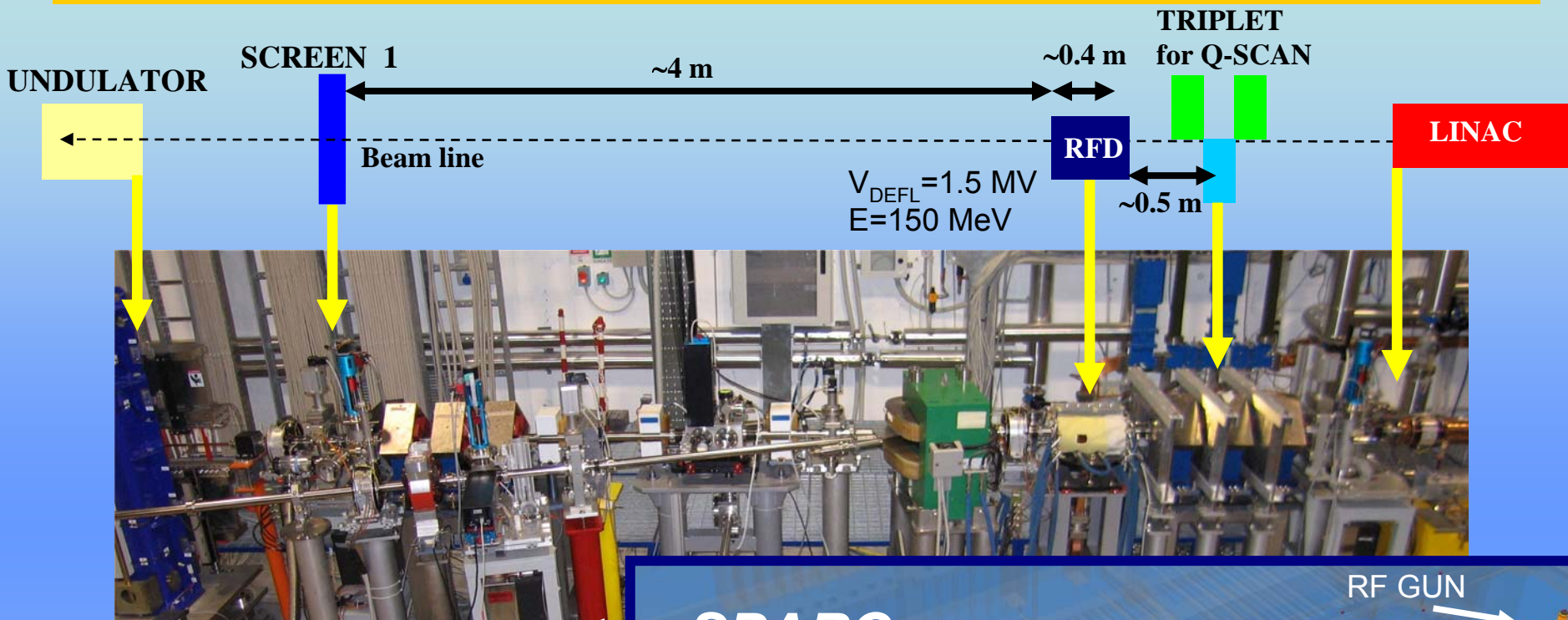
$$\begin{bmatrix} y_{out} \\ y'_{out} \\ t_{Bout} \\ \left. \frac{dp}{p} \right|_{out} \end{bmatrix} = \begin{bmatrix} 1 & L_{RFD} & 1/2 BL_{RFD}^2 & 1/2 CL_{RFD}^2 \\ 0 & 1 & BL_{RFD} & CL_{RFD} \\ 0 & 0 & 1 & 0 \\ \underbrace{DL_{RFD} \quad 1/2 DL_{RFD}^2}_{M_{RFD}} & 0 & 0 & 1 \end{bmatrix} \begin{bmatrix} y_{in} \\ y'_{in} \\ t_{Bin} \\ \left. \frac{dp}{p} \right|_{in} \end{bmatrix}$$

$$D = -\frac{E_{defl} \omega_{RF}}{c E_B} \sin(\phi_{RF})$$

Energy variation due to the
longitudinal e-field off axis

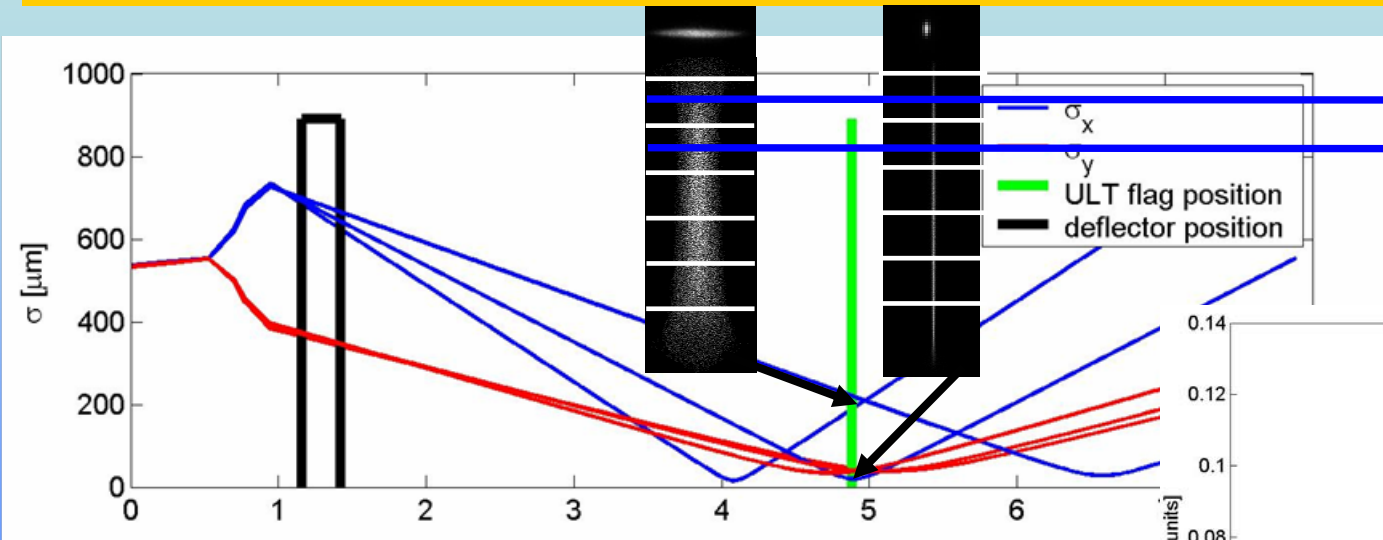


General meas. setup: beam profile and transverse slice emittance



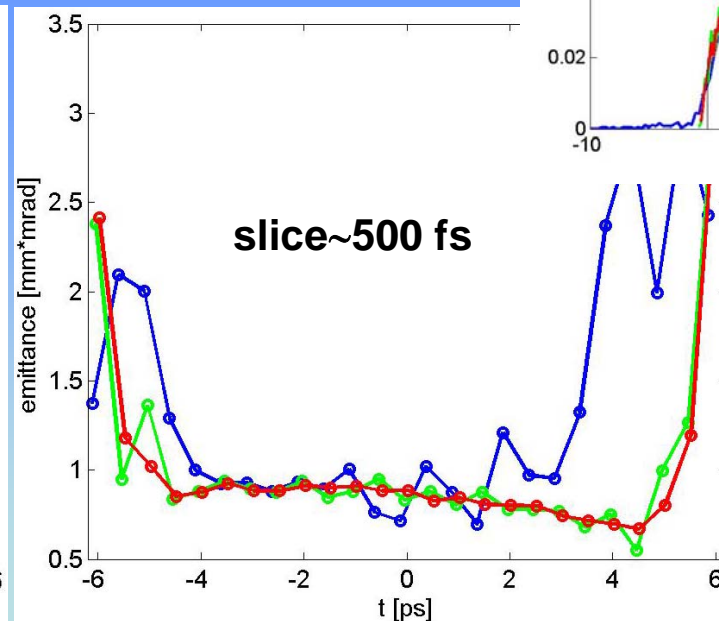
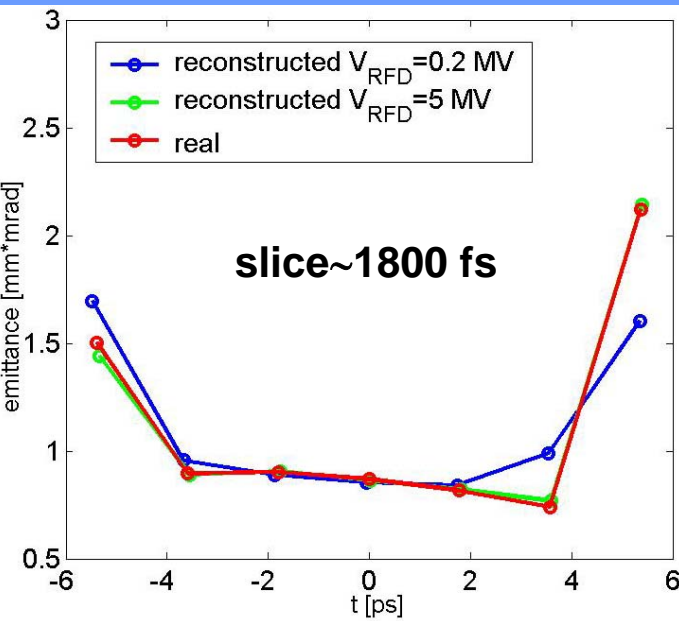
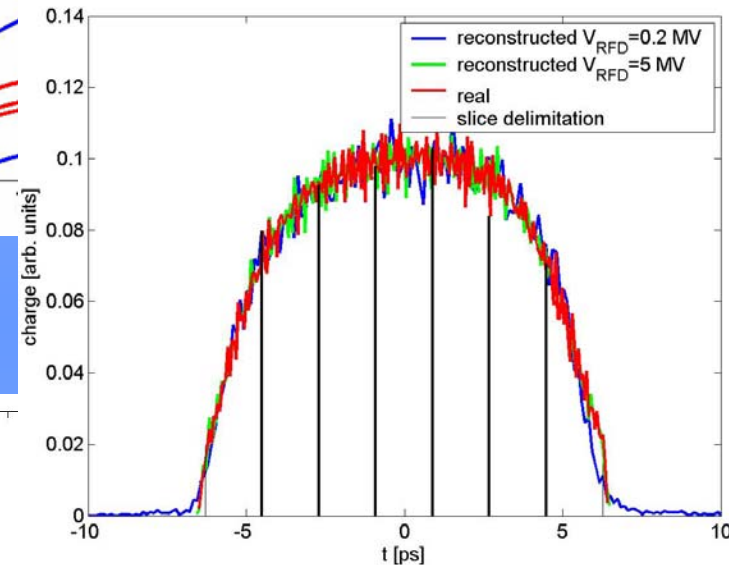
For beam profile and transv. slice emittance the beam image is taken on the screen 1. The slice beam emitt. is measured by the quad.scan.

Transverse slice emittance and beam profile: virtual measurement



Q-scan for each slice

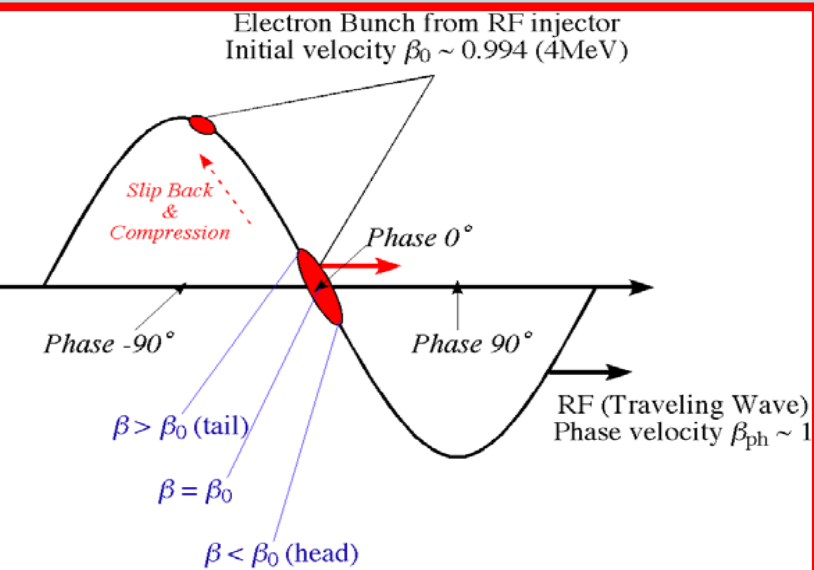
A set of values for the quadrupoles must be found in advance to change only the horizontal dimension of the beam, **keeping constant the vertical size** in order to have the same longitudinal resolution.



$$\sigma_{t_B-RES} @ 0.2MV \cong 400 fs$$

$$\sigma_{t_B-RES} @ 5MV \cong 15 fs$$

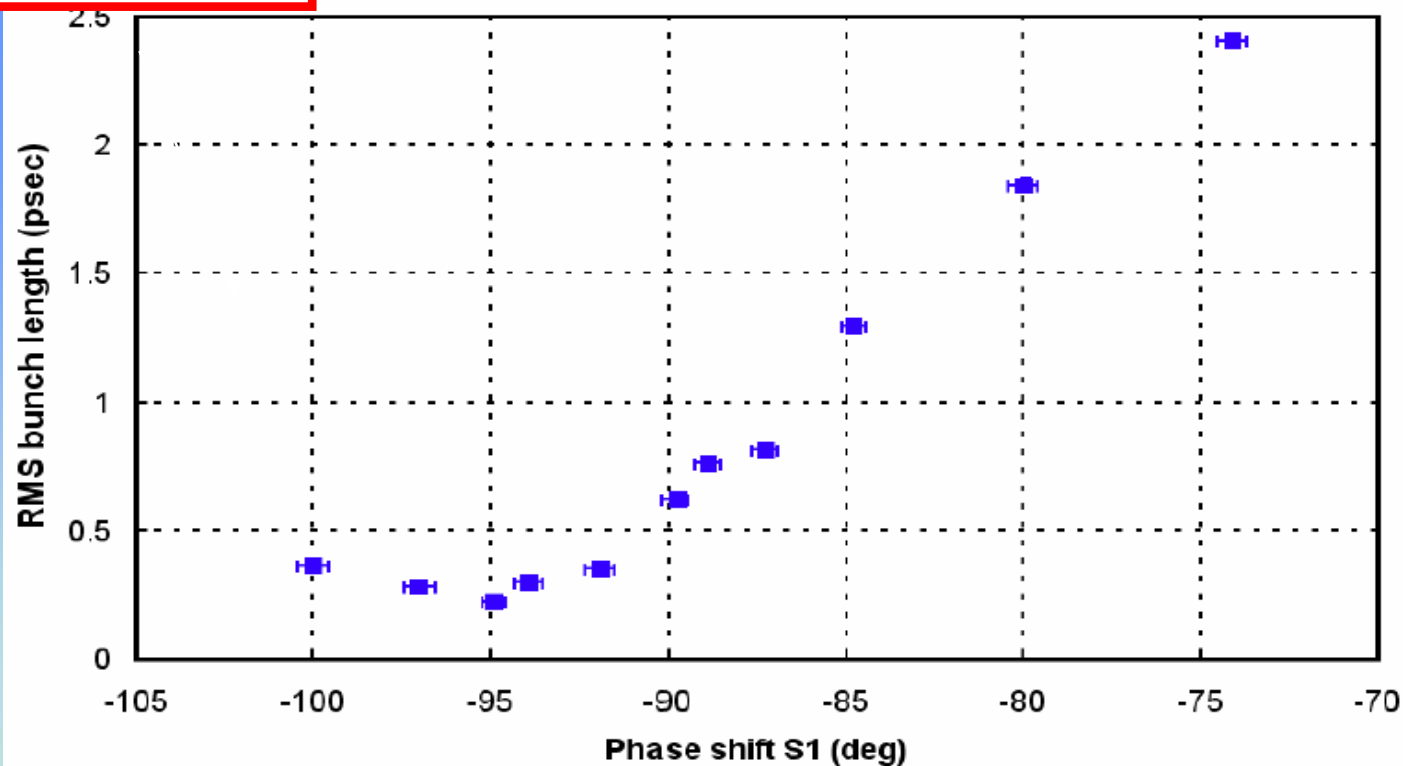
Beam profile measurements: measurement@SPARC (1/2)



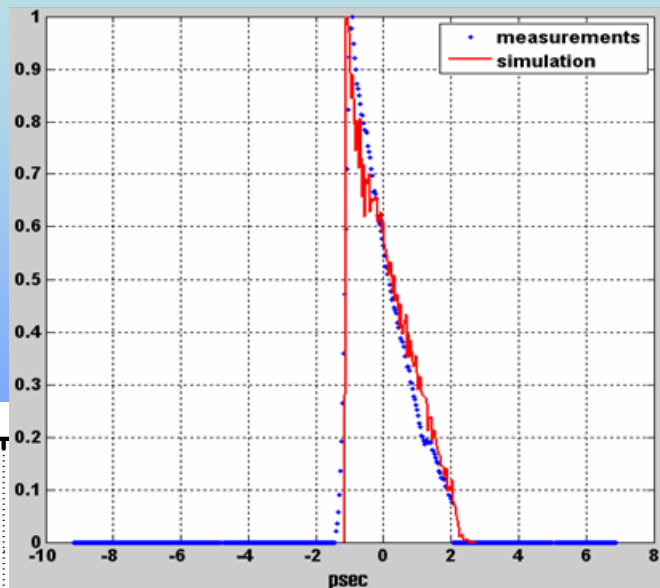
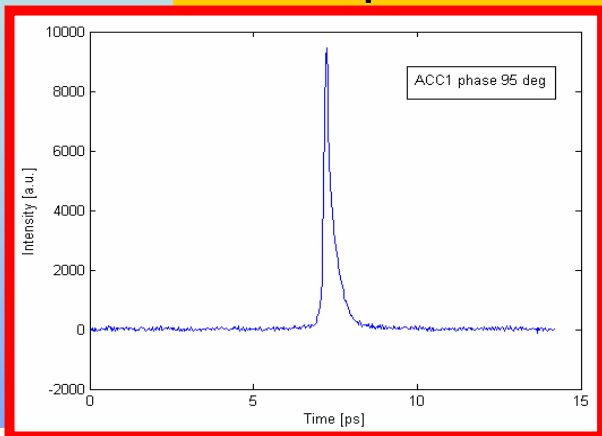
VELOCITY BUNCHING MEASUREMENTS

If the beam injected in a long accelerating structure at the crossing field phase and it is slightly slower than the phase velocity of the RF wave, **it will slip back to phases where the field is accelerating, but at the same time it will be chirped and compressed.**

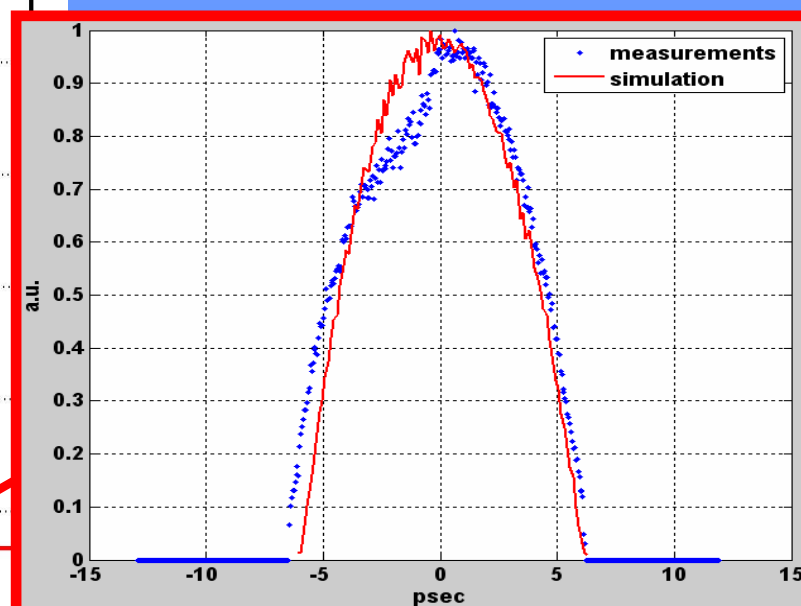
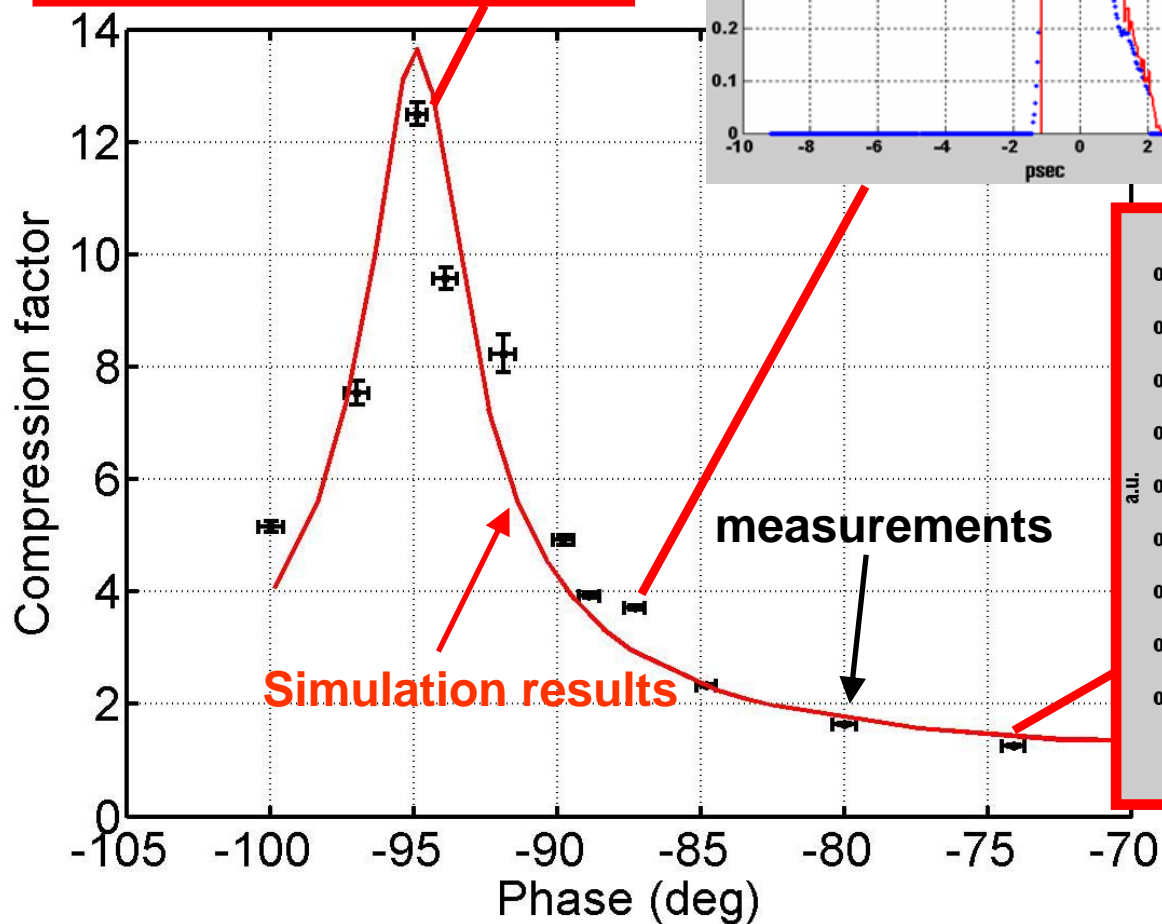
We operated with a **quasi-Gaussian long-laser profile** ~ 7.5 ps FWHM long with 300 mm transverse spot size and 300 pC. The beam acceleration on crest corresponds to the phases around -75 deg. In this condition bunch length is length measured at the linac exit was 2.5 ps with an energy of 150 MeV.



Beam profile measurements: measurement@SPARC (2/2)

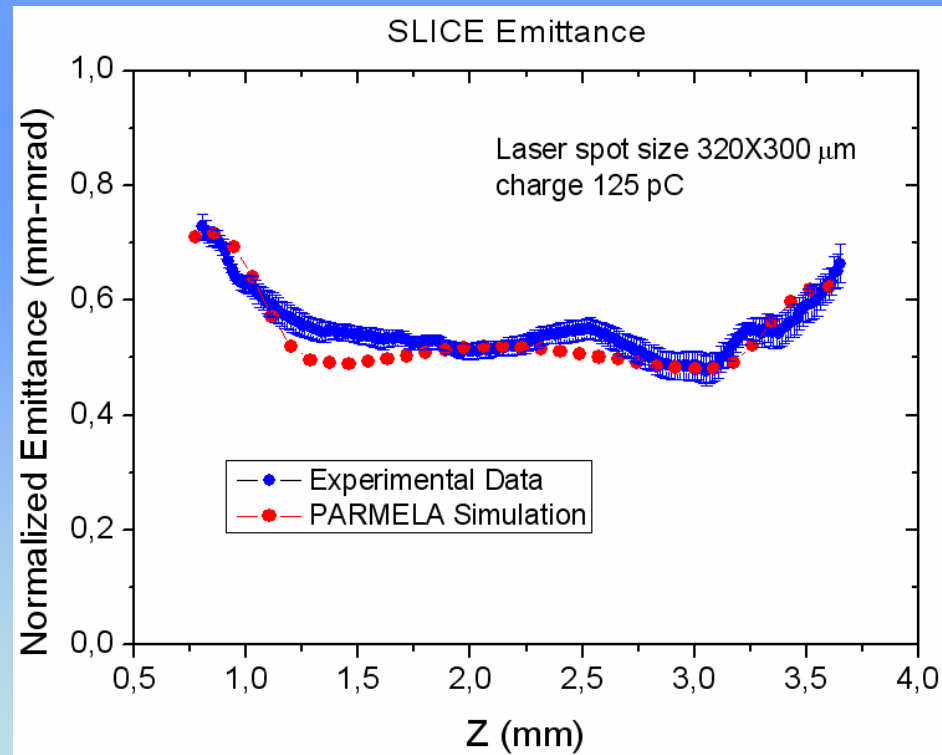
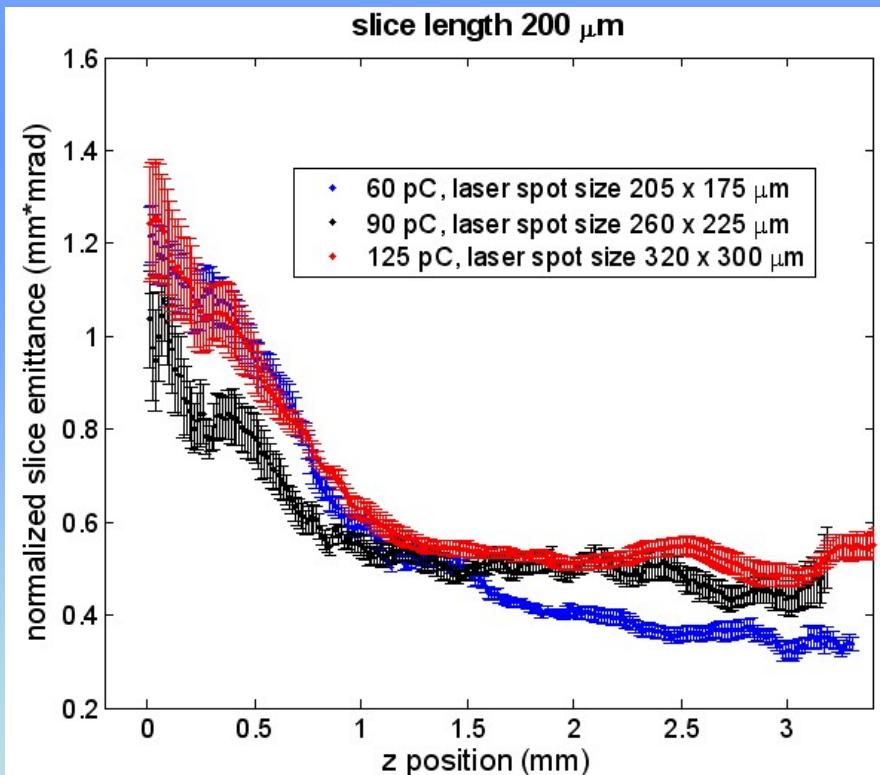


The longitudinal beam profile measurements are crucial for this experiment because, **while the bunch is compressed, it also change its longitudinal distribution.**

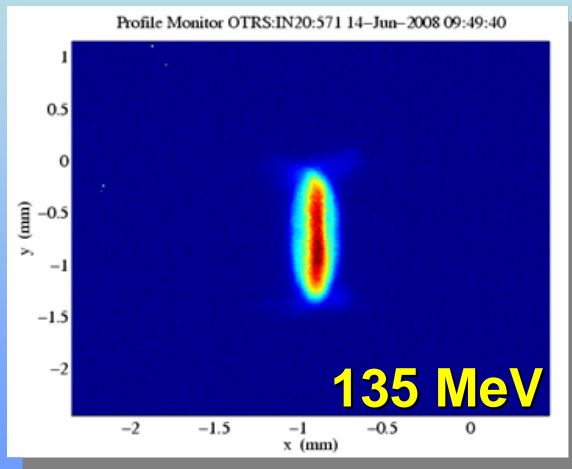


Transverse slice emittance: measurement@ SPARC

We compare the **slice emittance measurement** with a beam with **125 pC of charge** and a **laser spot on the cathode of 320X300 μm** with a **PARMELA simulation**. We used a technique that we called **RUS (Running Slice)**. It is very hard, especially on the beam tails, to determine the first and the last slice. This assumption however has impact on the position of all the other slices. To overcome this problem and resolve the ambiguity we fix a slice length (in our case 200 μm) and move it along the bunch in smaller steps.



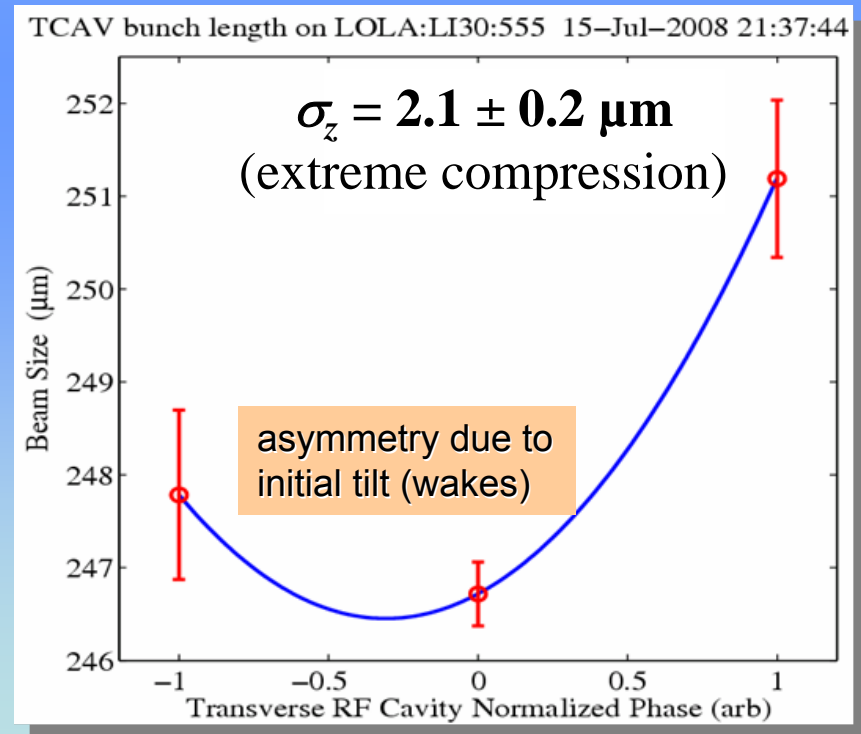
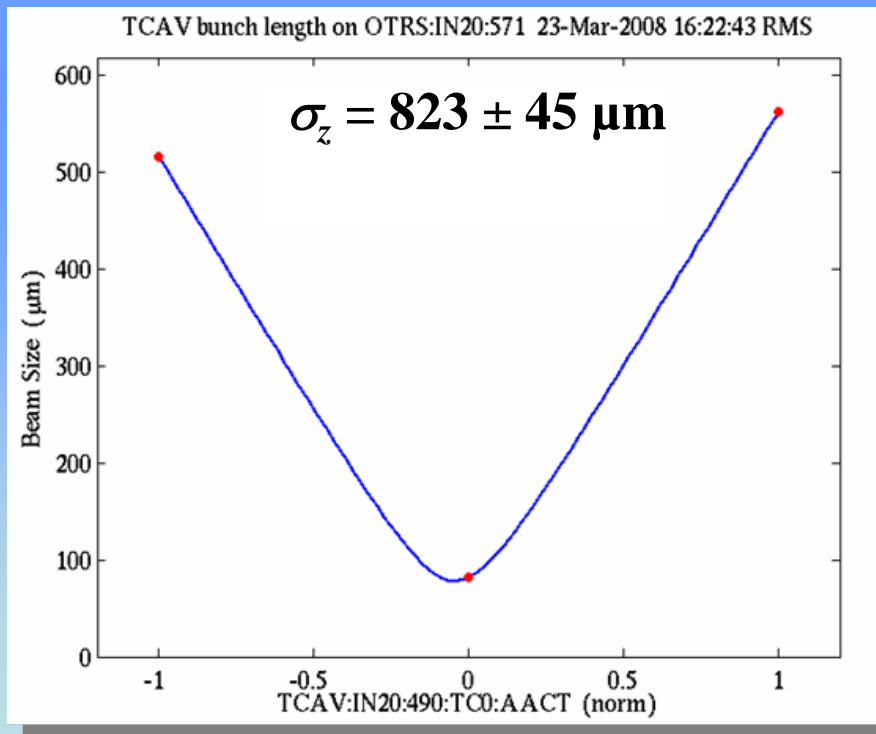
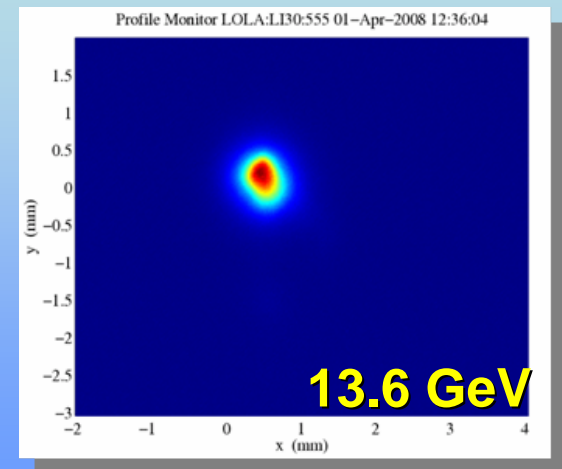
Beam profile: measurement@ LCLS (courtesy P. Emma)



Use Two Different Transverse RF Deflectors to Measure Bunch Length at 135 MeV and also at 13.6 GeV

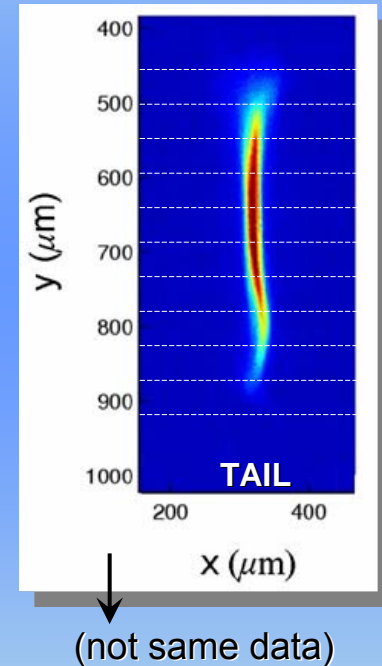
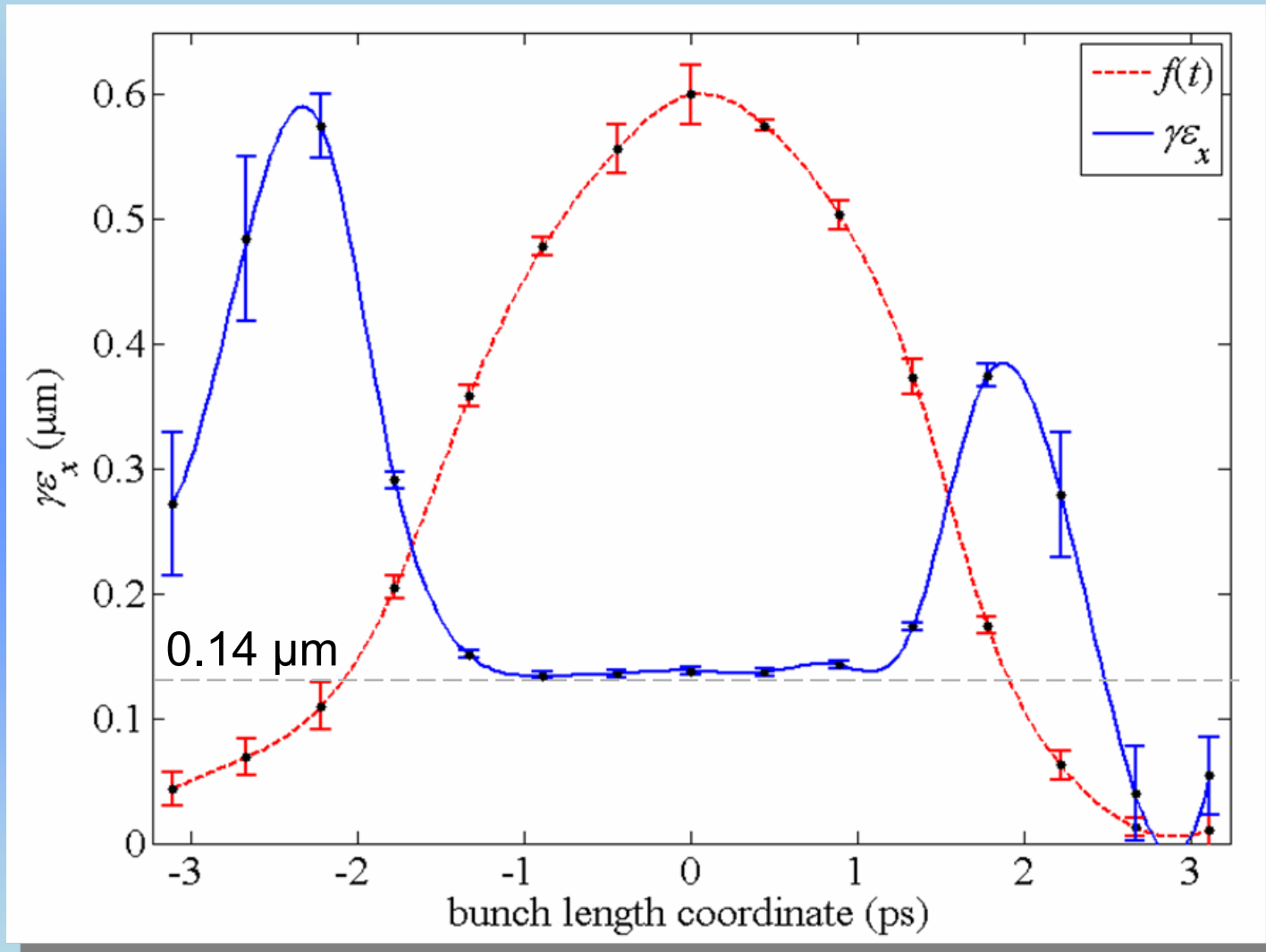
TW Structure (LOLA CAVITY)

$V_{\text{RFD}} \geq 15 \text{ MV}$
 $f_{\text{RF}} = 2.856 \text{ GHz}$



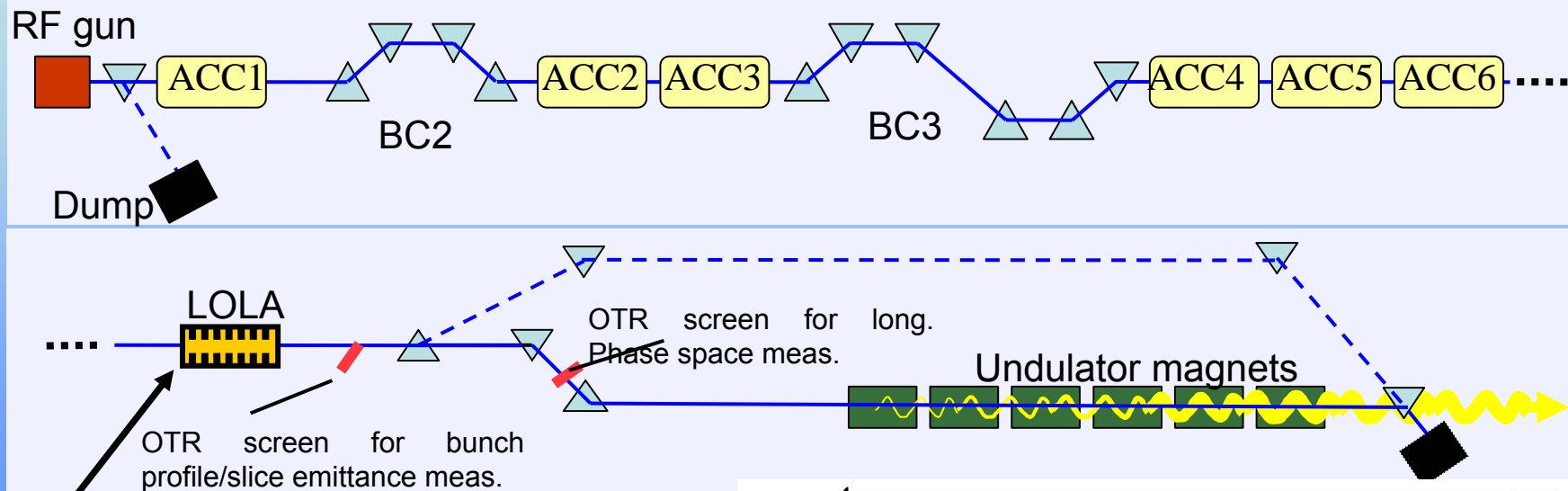
Transverse slice emittance: measurement@ LCLS (courtesy P. Emma)

Use Transverse RF to Measure Time-sliced Emittance at Low Charge

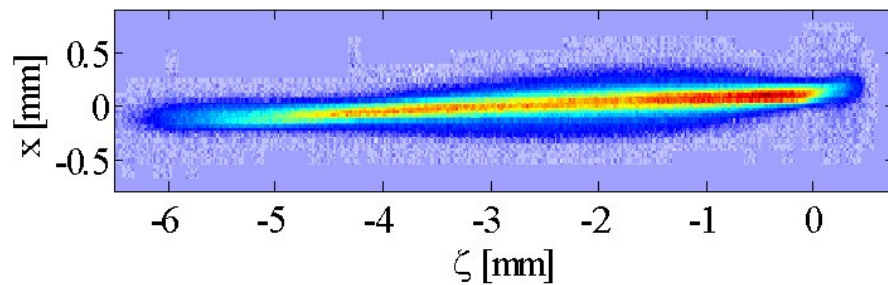
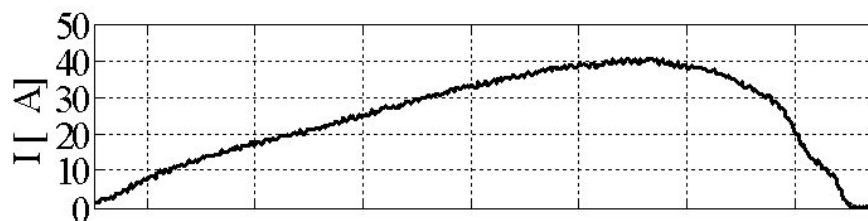
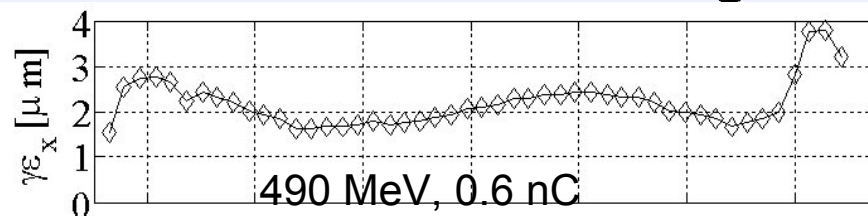


20 pC, 135 MeV, 0.6-mm laser spot diam., 400 μm rms bunch length (5 A)

Beam profile: measurement@FLASH (courtesy C. Gerth)

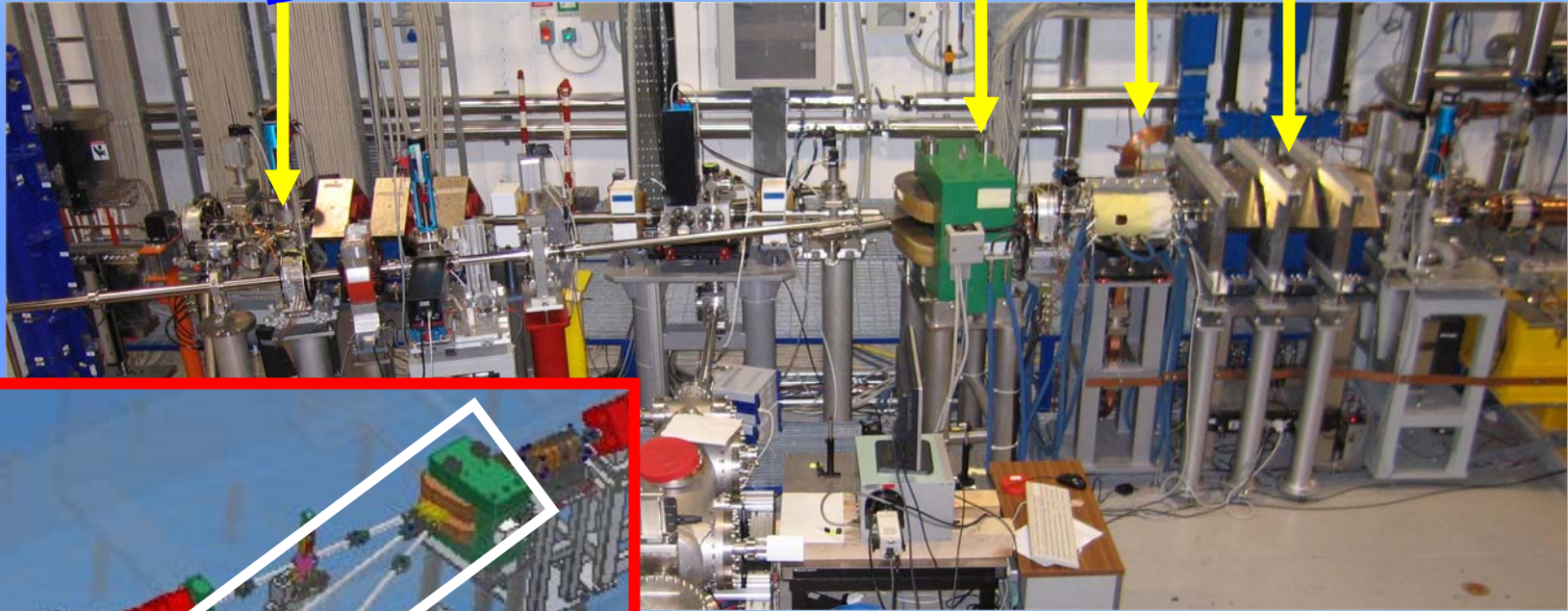
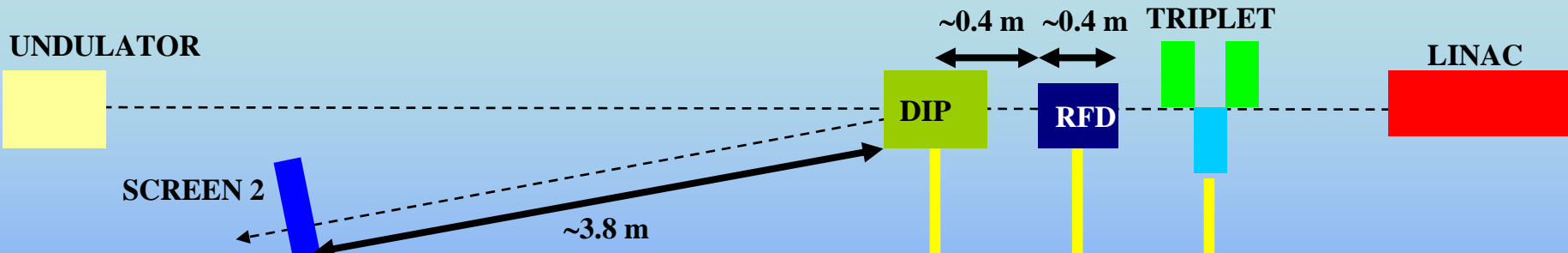


Frequency: 2.856 GHz
 Length: 3.6 m
 VRFD~25 MV@20 MW P_{IN}
 σ_{tB_RES} =20fs



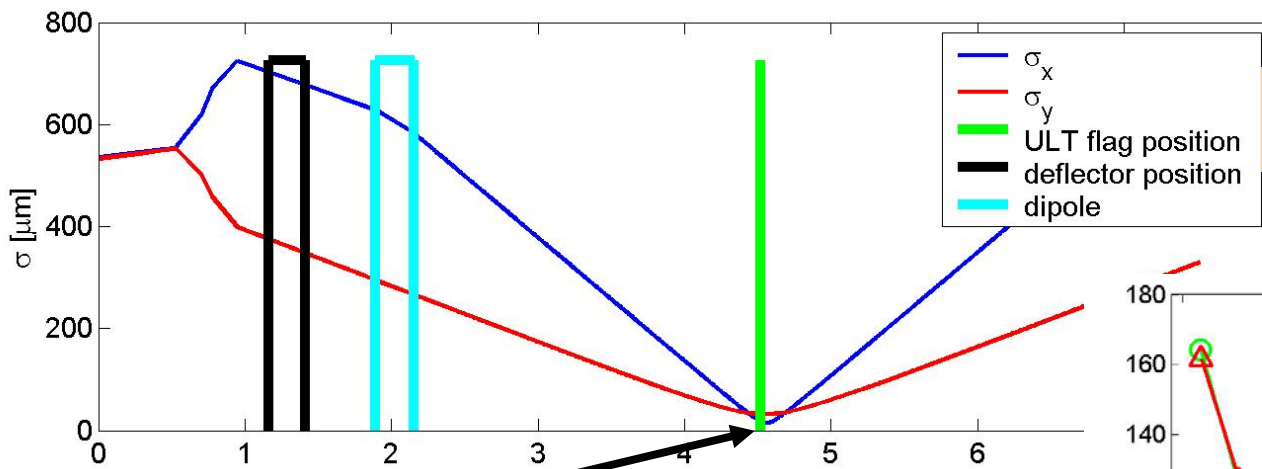
On-crest operation

General measurement setup: longitudinal phase space

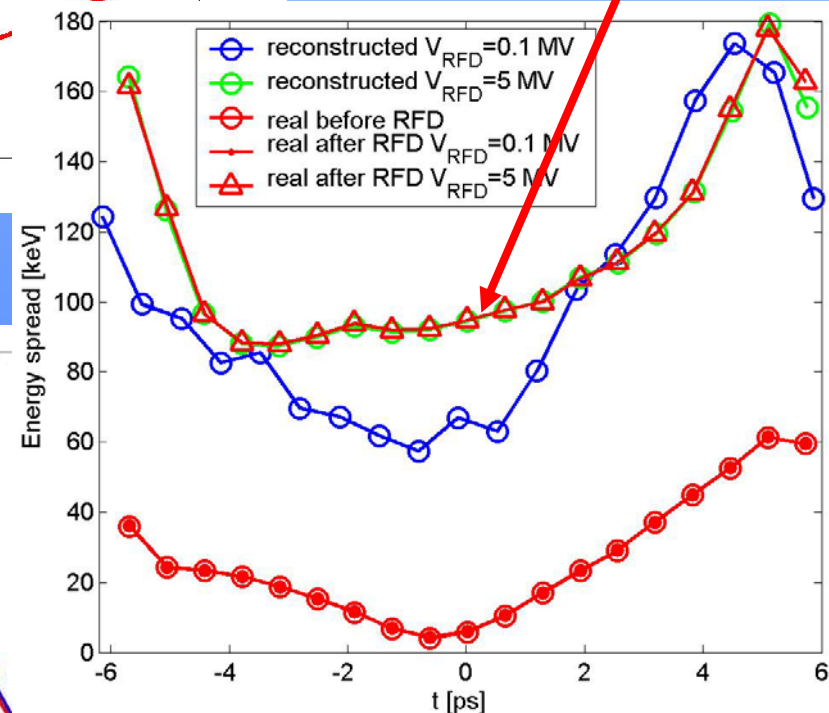
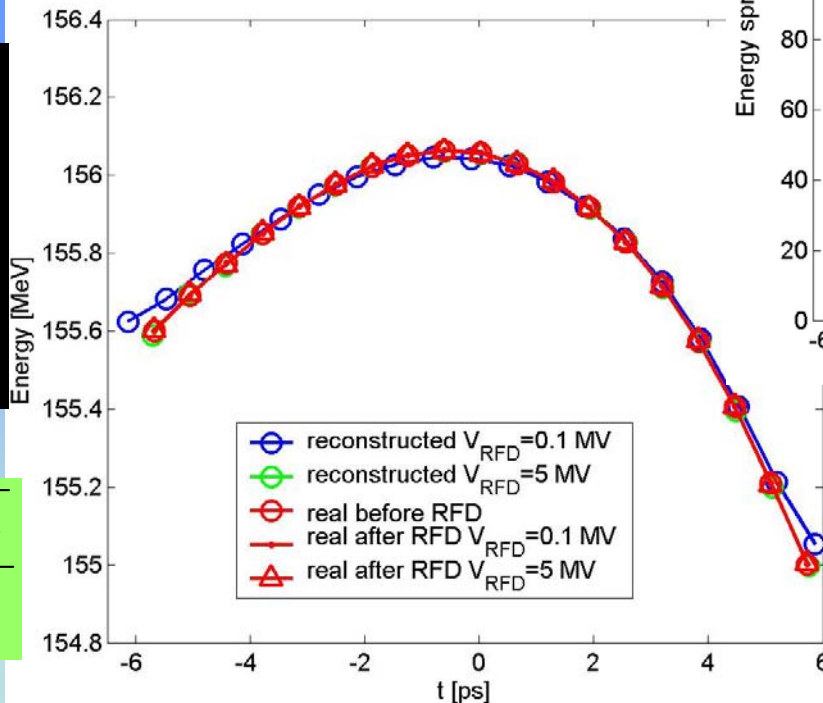
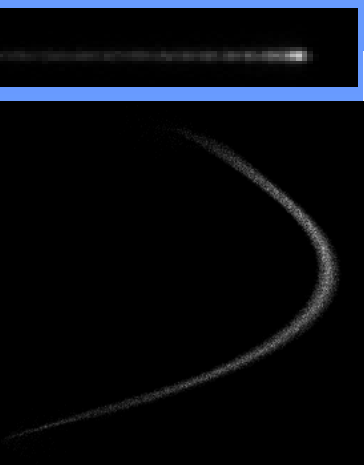


The longitudinal phase space can be characterized using the combination of RFD and dipole. In this case the beam is projected into the screen 2. In order to have enough longitudinal resolution the **vertical dimension at the screen position has to be taken under control**. From the phase space picture the slice energy spread can be extrapolated by slicing the beam vertically and measuring the beam thickness in energy as function of time.

Long phase space: virtual measurement



$$\sigma_{E_RFD} \cong \frac{\omega_{RF}}{C} \hat{V}_{y_RFD} \sigma_{y_RFD} = 107 [keV]$$



Also the horizontal β -function at the screen has to be reduced as much as possible in order to reduce the emittance contribution to the energy spread measurement. **In any case the dominant systematic error is the energy spread induced by the RFD**

$$\left. \frac{\Delta E}{E} \right|_{\text{emitt}_{\text{res}}} = \frac{\sqrt{\epsilon \beta_{H_S}}}{D_S}$$

Long phase space: subtraction of the RFD contribution to σ_E

For each slice

$$\sigma_E^2 + \sigma_{E_RFD}^2 = \sigma_{E_MIS}^2 \Rightarrow \begin{cases} \sigma_E^2 + \sigma_{E_RFD_1}^2 = \sigma_{E_MIS_1}^2 \\ \sigma_E^2 + \sigma_{E_RFD_2}^2 = \sigma_{E_MIS_2}^2 \end{cases}$$

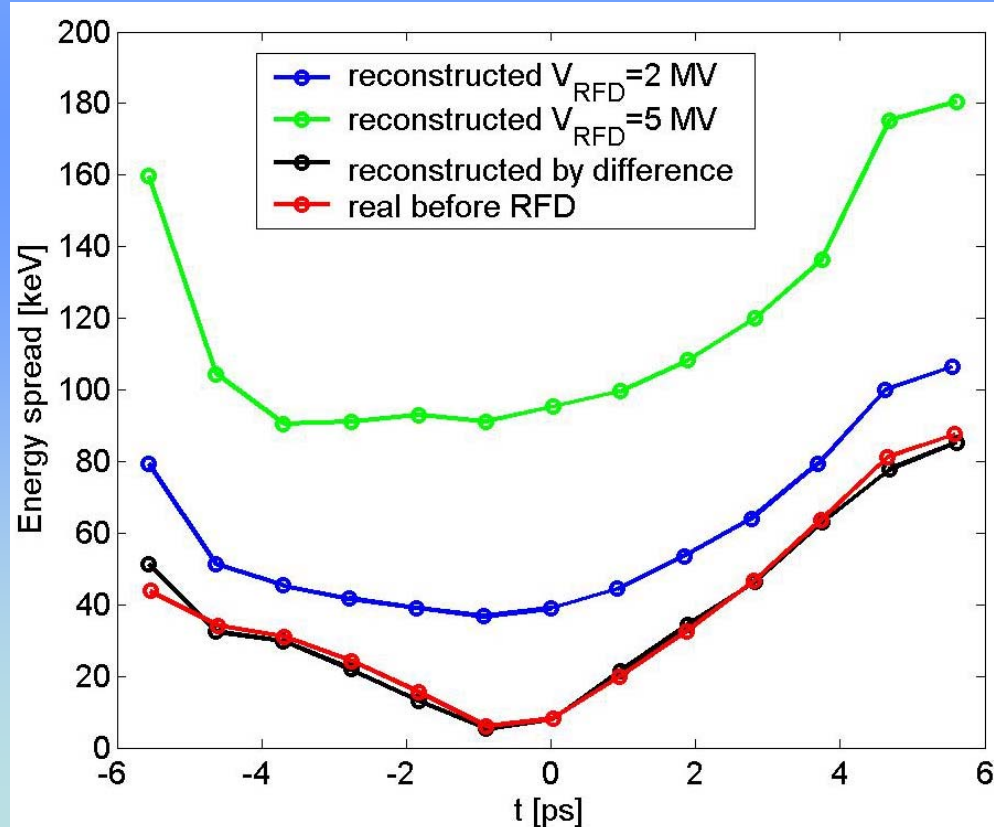
$$\left(\frac{\omega_{RF}}{c} \hat{V}_{DEFL_1}\right)^2 \sigma_{y_RFD}^2 - \left(\frac{\omega_{RF}}{c} \hat{V}_{DEFL_2}\right)^2 \sigma_{y_RFD}^2 = \sigma_{E_MIS_1}^2 - \sigma_{E_MIS_2}^2$$

$$\sigma_{y_RFD}^2 = \left(\frac{c}{\omega_{RF}}\right)^2 \frac{\sigma_{E_MIS_1}^2 - \sigma_{E_MIS_2}^2}{\hat{V}_{DEFL_1}^2 - \hat{V}_{DEFL_2}^2}$$

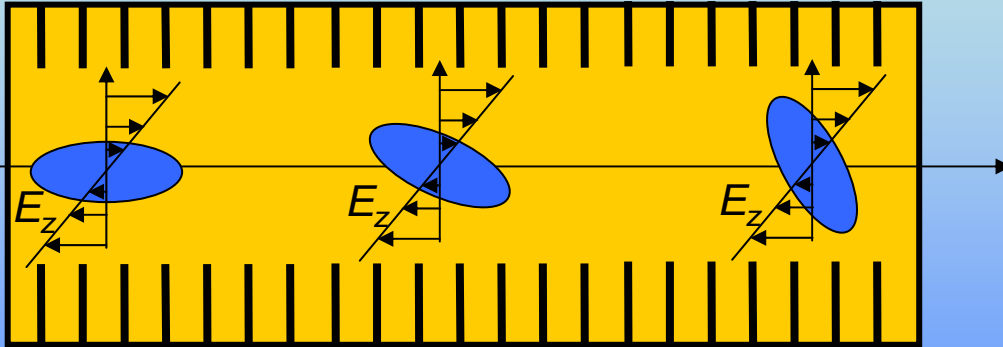
$$\sigma_{E_RFD} \cong \frac{\omega_{RF}}{c} \hat{V}_{DEFL} \sigma_{y_RFD} \quad [eV]$$

$$\sigma_E^2 = \sigma_{E_MIS}^2 - \sigma_{E_RFD}^2$$

The contribution of the deflector to the slice energy spread can be taken into account performing two measurements at two different deflecting voltages and using the following formulae to evaluate the sigma σ_{yB_RFD} of each slice.

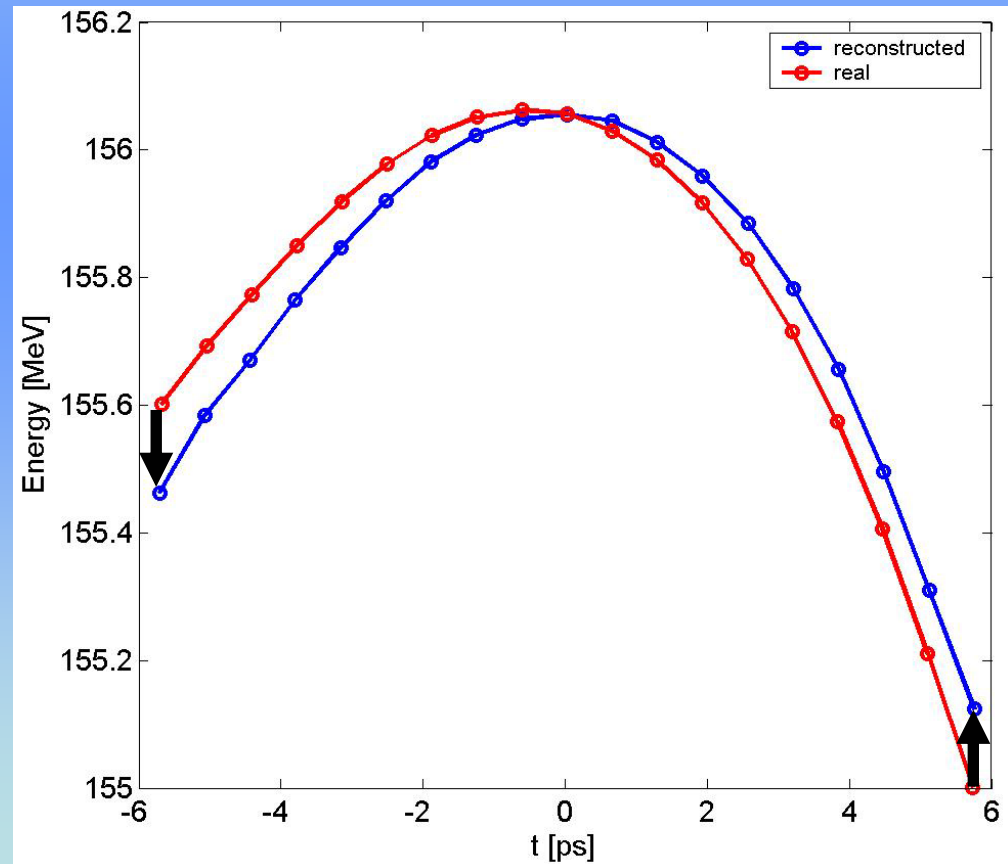


Long phase space: effect of long RFD structures

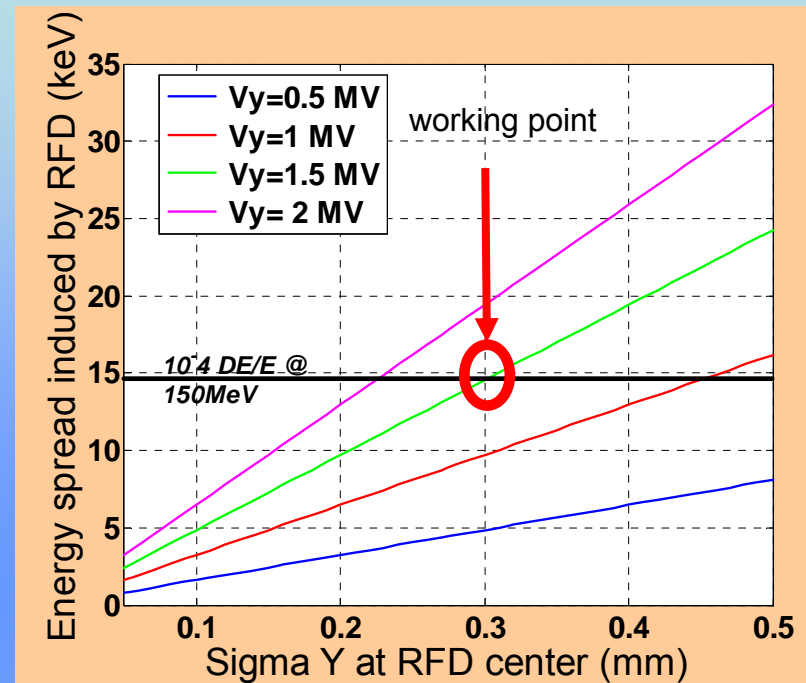
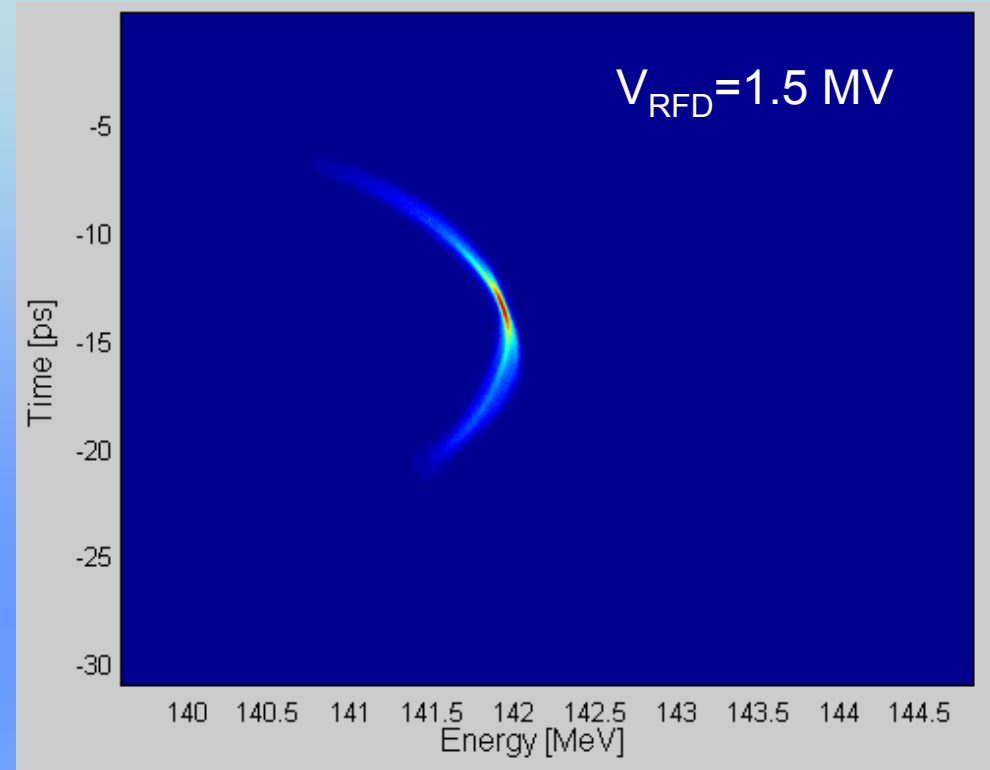


If we consider a long RFD, we can have effects also on the measured average energy of each slice because the bunch head-tail rotate along the deflector and experience a non-zero average electric field

Example:
Assuming a $L_{\text{RFD}} = 0.8 \text{ m}$ @ SPARC

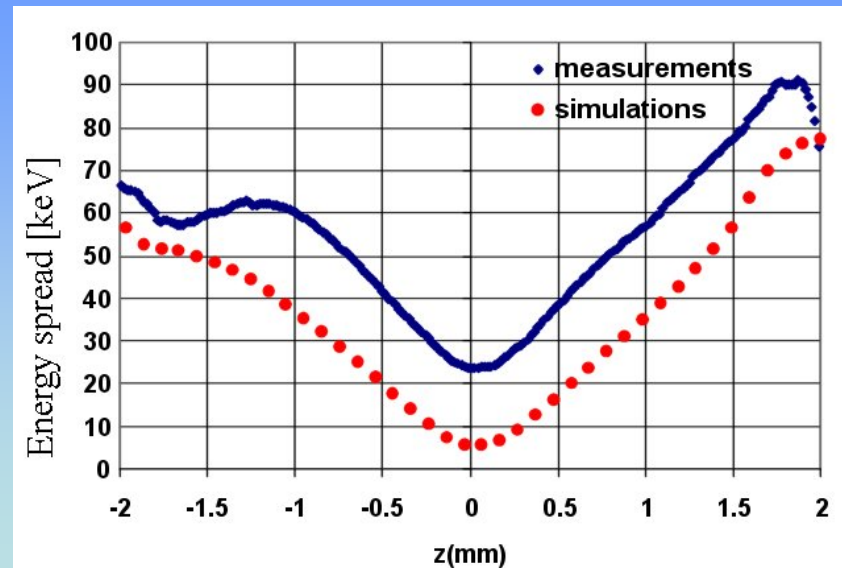


Long phase space: measurement @ SPARC

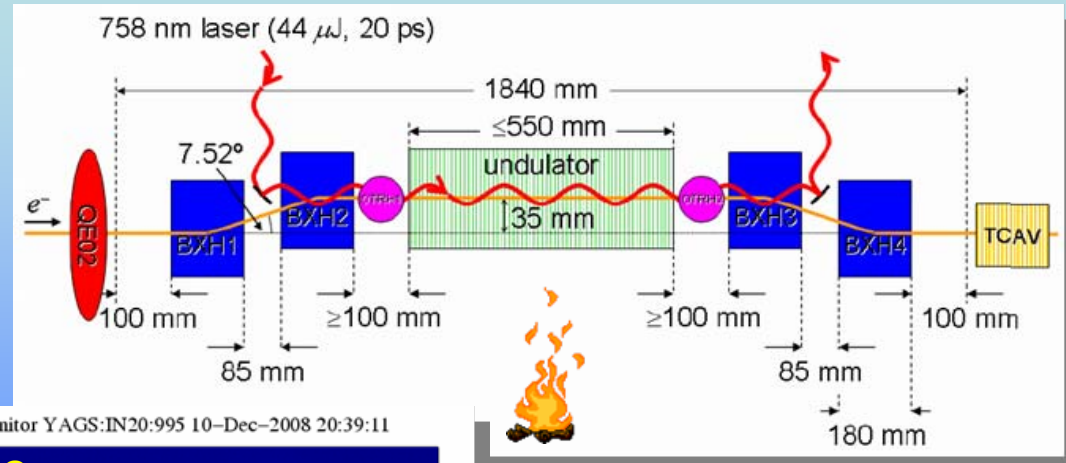
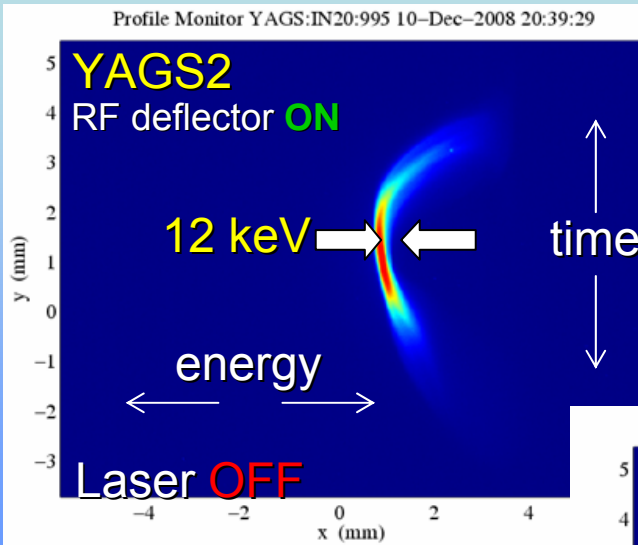


From the plot the slice energy spread can be extrapolated and compared with simulations. The main discrepancy between the simulations and the experimental data is given by the **RFD contribution** that has been estimated to be $\sim 15 \text{ keV}$.

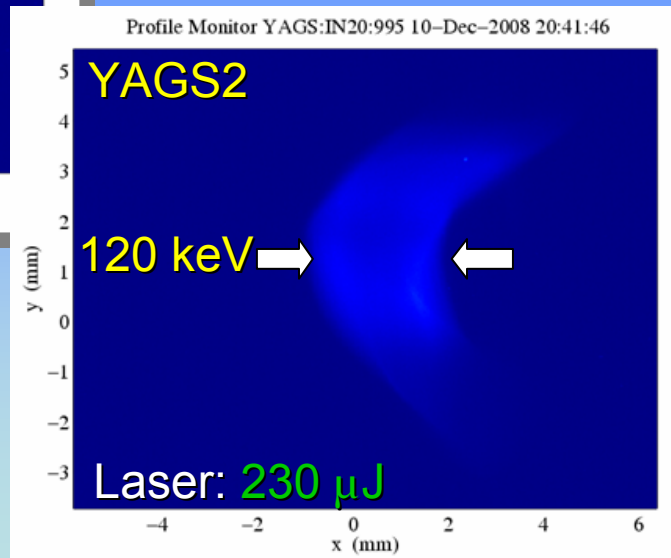
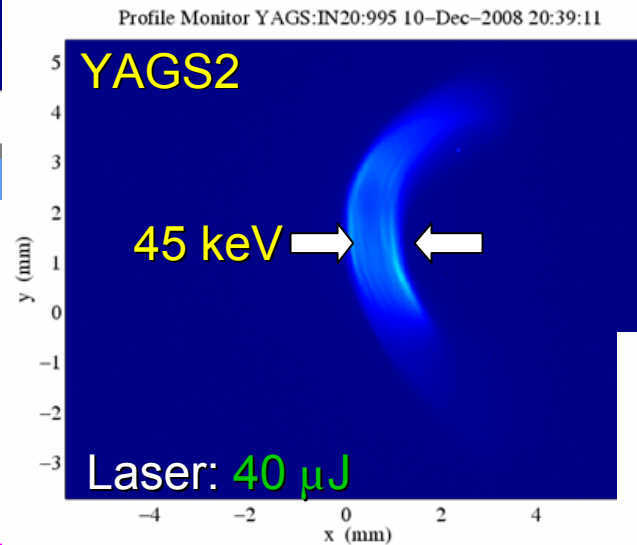
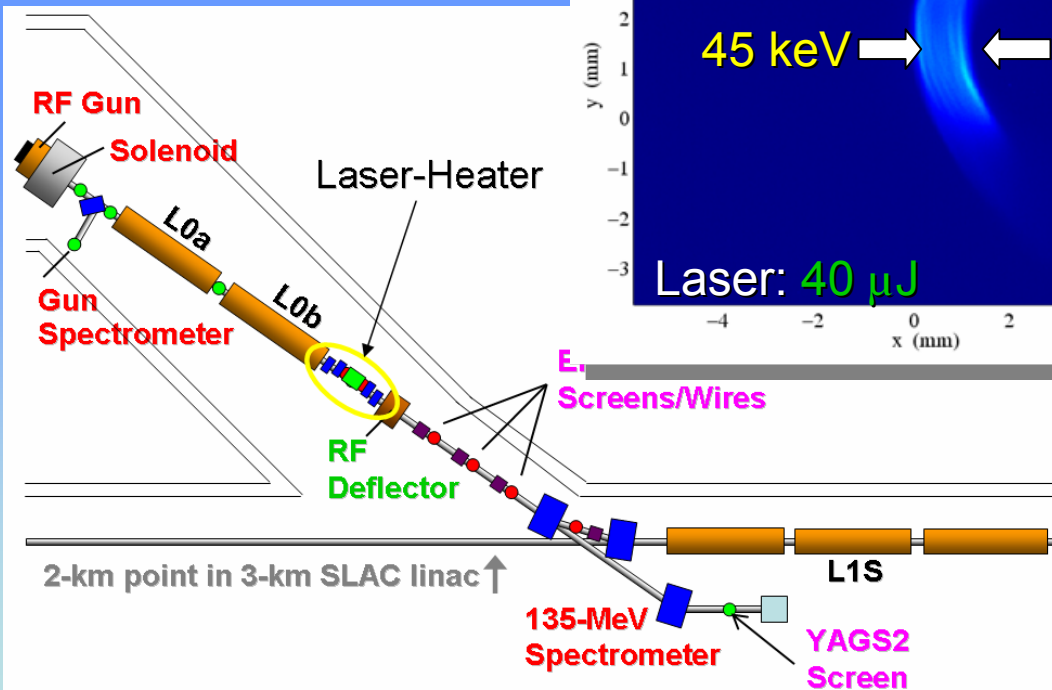
The **emittance contribution** has not been subtracted from the measurements, but it has been estimated to be less than 10%.



Long phase space: measurement @ LCLS (courtesy P. Emma)



Use Transverse RF to measure sliced E -spread of "Laser-Heater"



Long phase space: measurement @ LCLS (courtesy P. Emma)

Use Transverse RF to Verify Compression Linearization of X-Band RF (11.4 GHz)

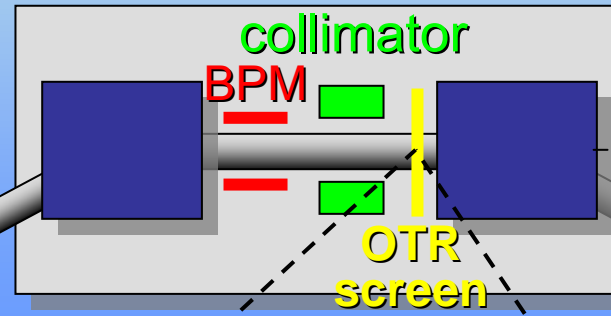
LCLS
measurements

$L = 0.6$ m

X-band

$V = 20$ MV

$\varphi = -160^\circ$

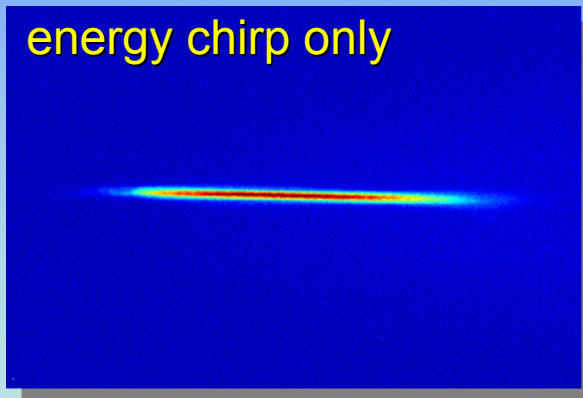


Offset: 0 to 300 mm
(247 mm nominal)

measurements

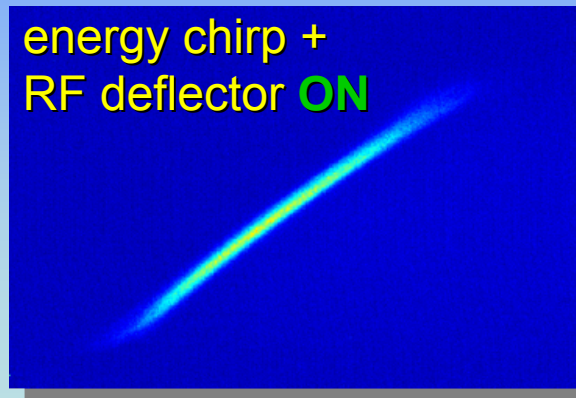
RF deflector **OFF**

energy chirp only



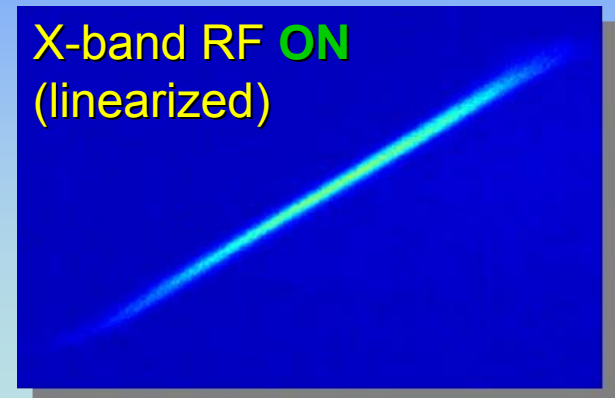
RF deflector **ON**

energy chirp +
RF deflector **ON**



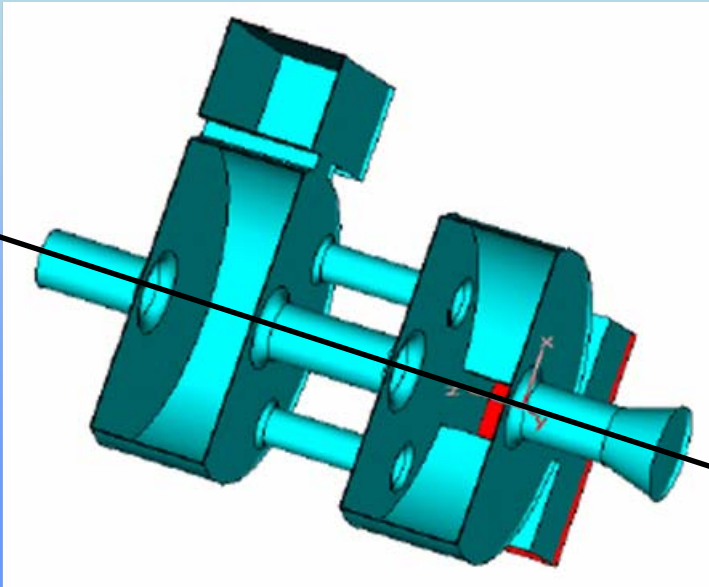
Deflector **ON** & X-band **ON**

X-band RF **ON**
(linearized)

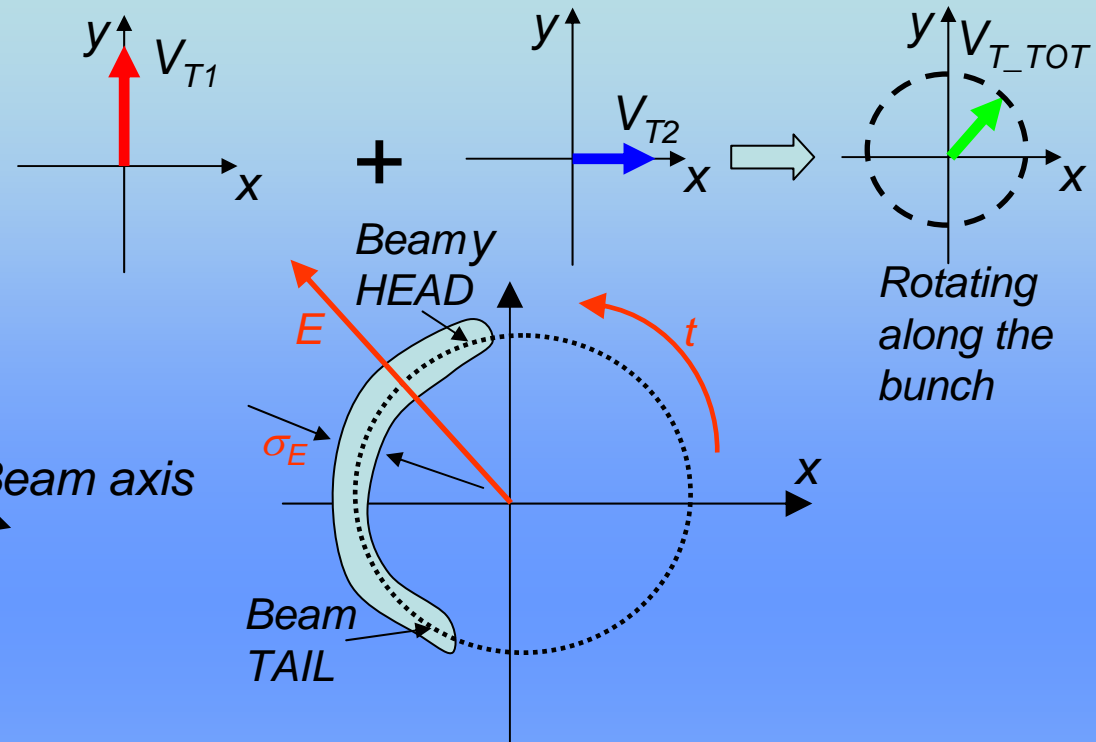


Advanced RFD structures: circular polarized RF deflector

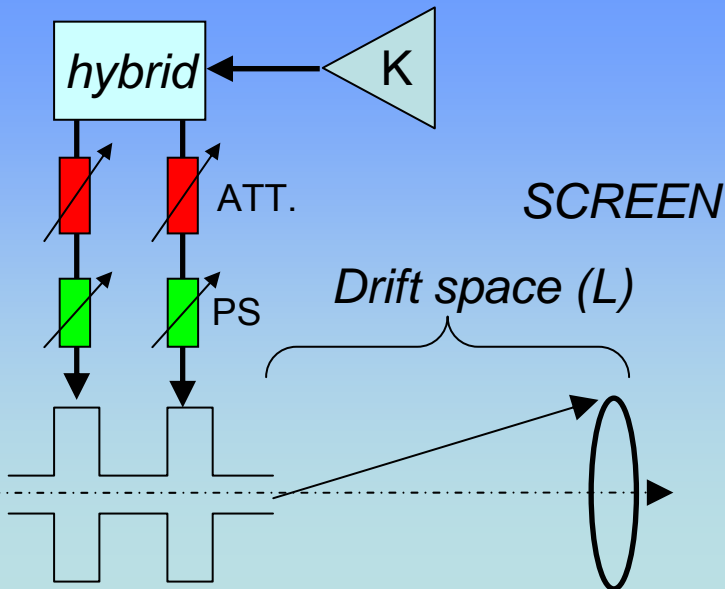
[Haimson et al, AIP, 647, 2002]



Beam axis



POWER SCHEMES



Longitudinal and energy spread resolutions

$$\sigma_{t_B-RES} = \frac{\sigma_B}{\frac{V_T}{E/e} \omega_{RF} L}$$

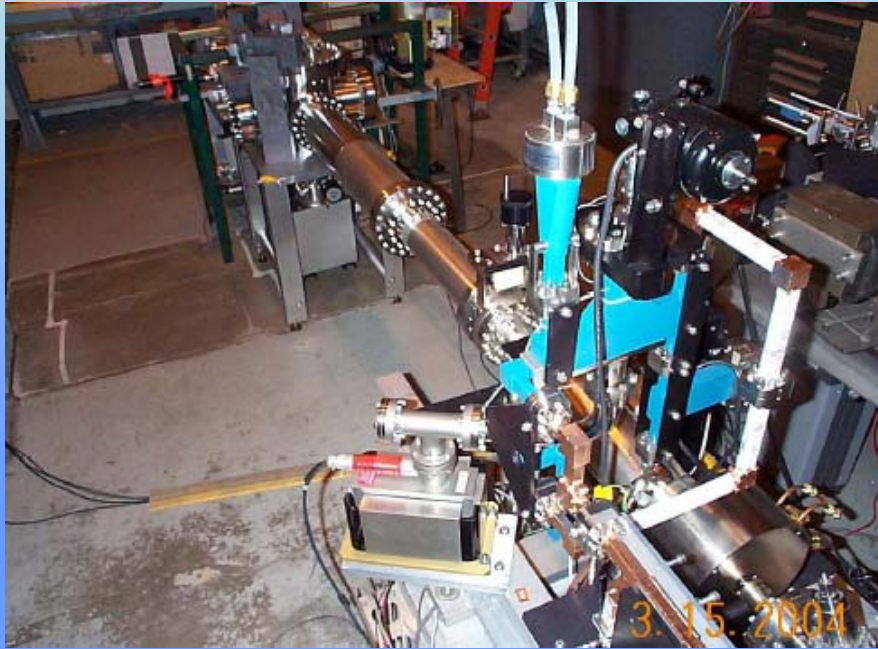
$$\left. \frac{\Delta E}{E} \right|_{RES} = \frac{(E/e)\sigma_B}{V_T L}$$

1	L_{RFD}	$1/2 B I_{RFD}^2$	$1/2 C L_{RFD}^2$
0	1	$B L_{RFD}$	$C L_{RFD}$
0	0	1	0
$D L_{RFD}$	$1/2 B L_{RFD}^2$	0	1

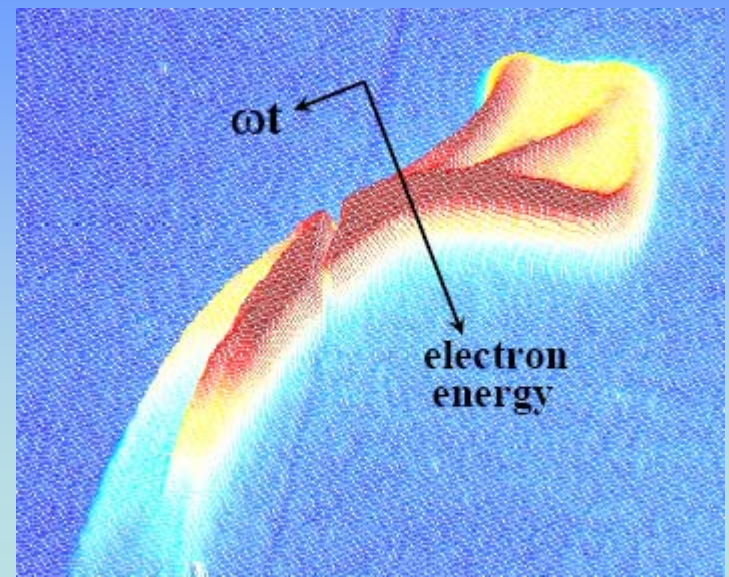
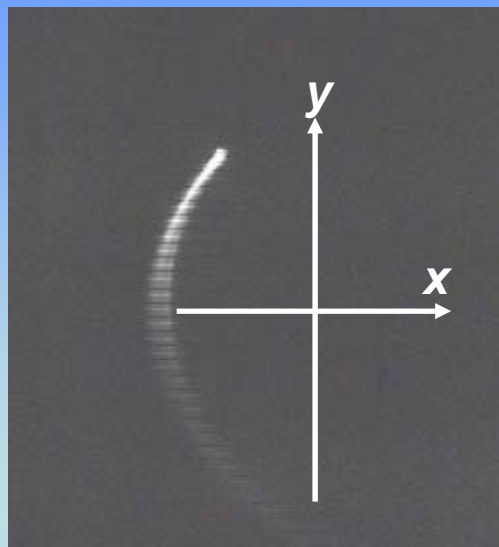
No energy spread induced by RFD!

Circular polarized RF deflectors: measurements

[J. Haimson et al, AIP, 737, 2004]

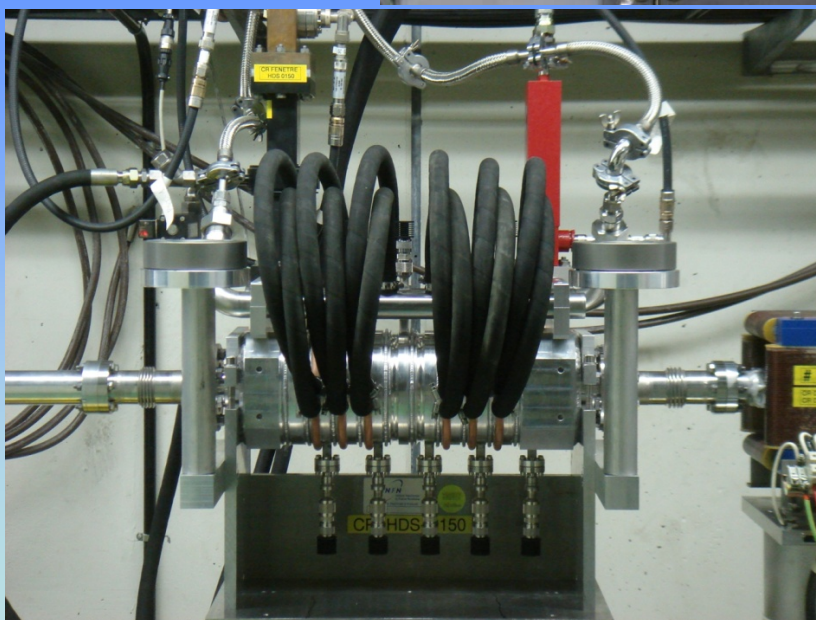
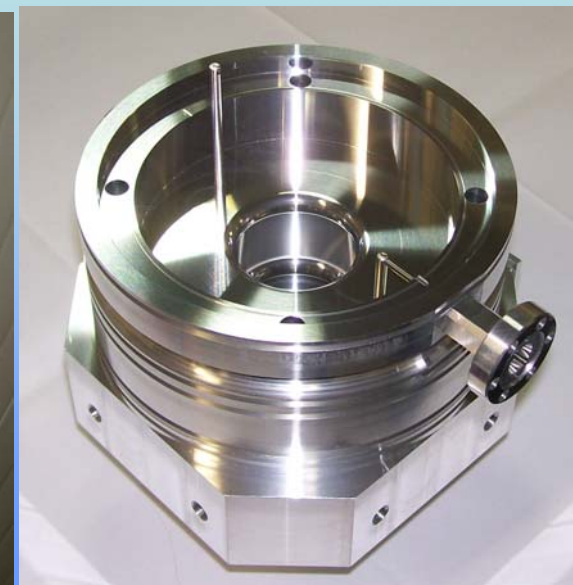
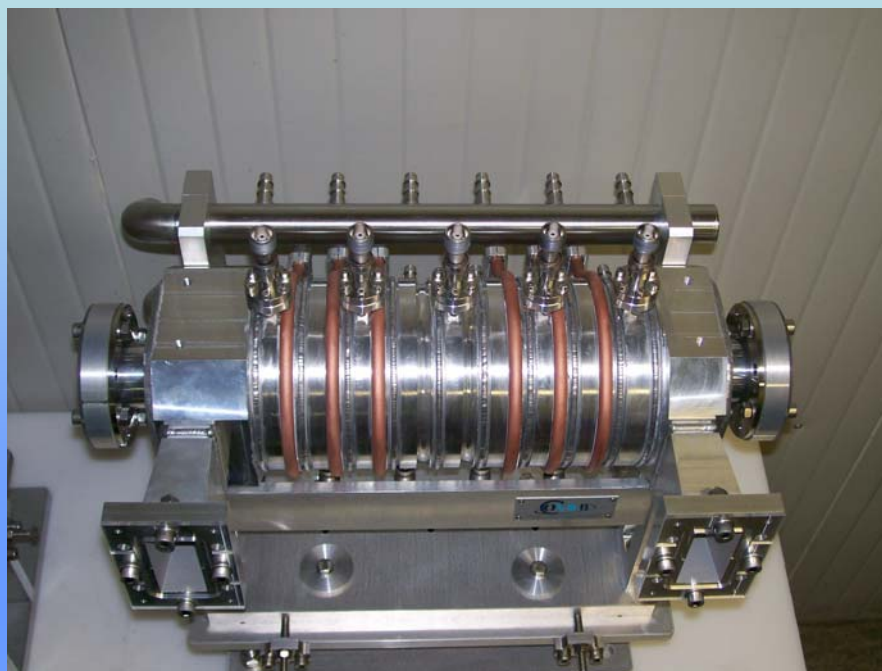


Number of Cavities	2
Operating Frequency	~ 17 GHz
Nominal Beam Energy	15 MeV
RF Deflection Angle	~ 27 mradian
Drift Distance	2 m
Beam Deflection @ Screen	57 mm
Peak RF Input Power	734 kW
Normalized Emittance	2.8π mm.mrad
Longitudinal resolution	~ 100 fs
Bunch length	~ 5 mm



Advanced RFD structures: Aluminum RF deflectors

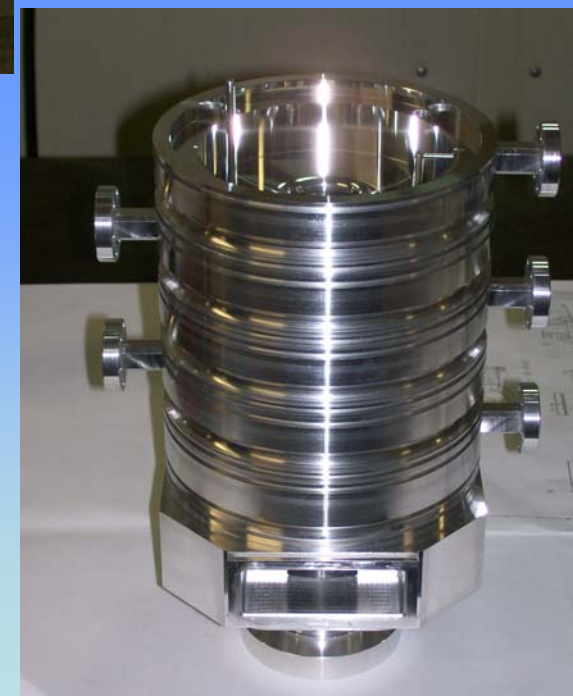
The new RFD of the **CTF3 Combiner Ring** have been built in aluminium to reduce the cost and the delivery.



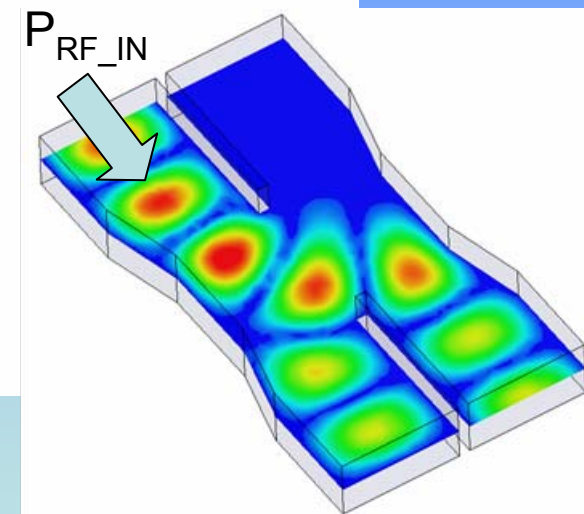
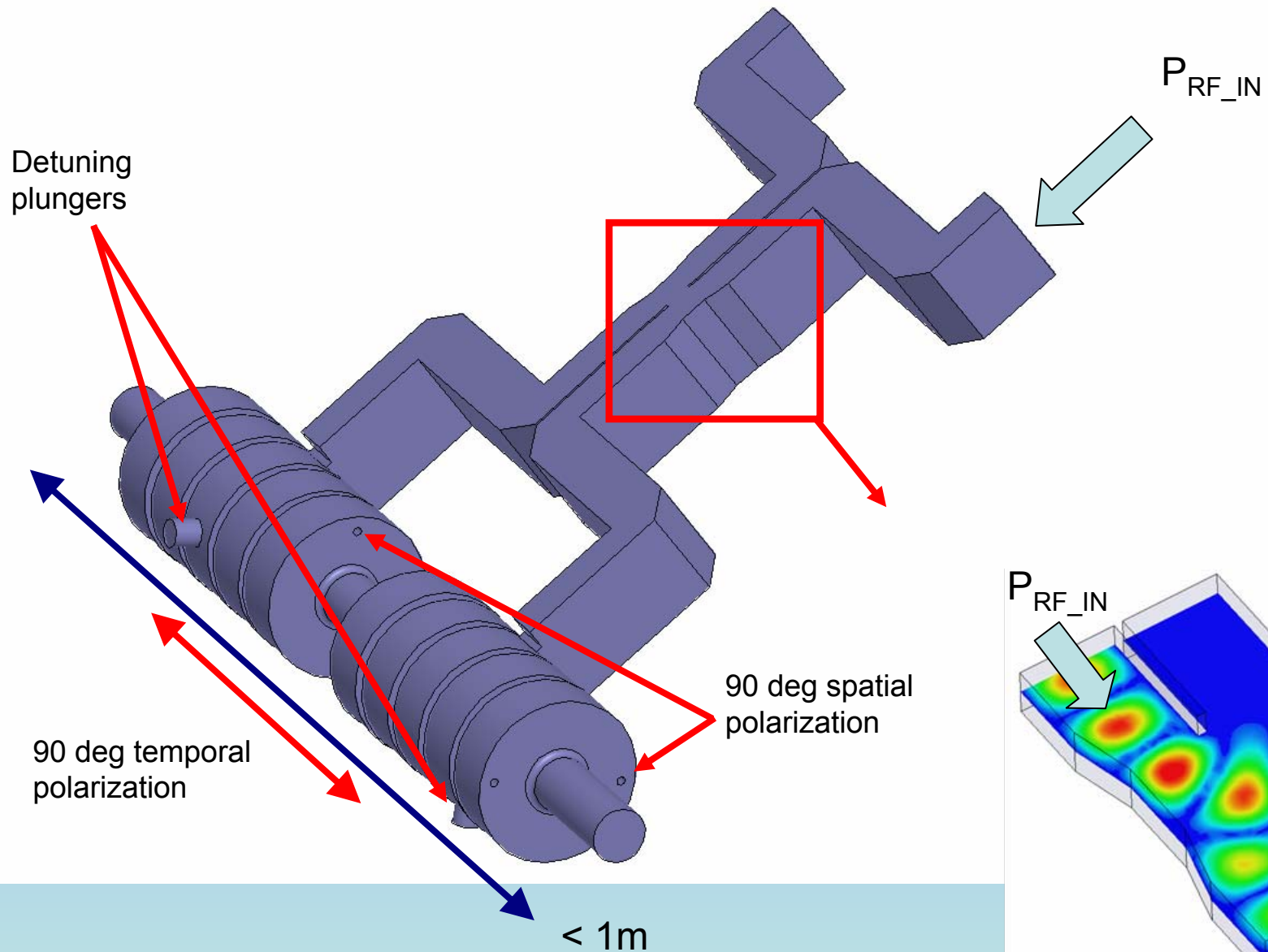
The cells have been machined, clamped together with tie rod to guarantee the RF contacts and welded.

The structure has been installed with success without observing MP phenomena.

D. Alesini et al., PAC 09.



The next generation RFD for beam diagnostics



CONCLUSIONS

RFDs are fundamental devices for both longitudinal and transverse phase space characterization allowing reaching **resolution below 10 fs**.

The measurement setups and the experimental results, in the **SPARC case**, have been shown and discussed.

In particular the use of the RFD technique has been fundamental in the **velocity bunching** experiment at SPARC.

A possible solution to **take into account the contribution of the RFD in the energy spread slice** has been also illustrated.

Important new results have been also reached in other accelerator facilities like **LCLS or FLASH**: the use of the RFD technique allowed measuring laser heating effects or longitudinal phase space correction using X-Band cavities.

New important results have been recently obtained **in RFD fabrication with aluminum**

THANK YOU